AEDC-TR-75-114
AFATL-TR-75-132

FLOW-FIELD STUDY ABOUT A HEMISPHERE-CYLINDER IN THE TRANSONIC AND LOW SUPERSONIC MACH NUMBER RANGE

PROPULSION WIND TUNNEL FACILITY
ARNOLD ENGINEERING DEVELOPMENT CENTER
AIR FORCE SYSTEMS COMMAND
ARNOLD AIR FORCE STATION, TENNESSEE 37389

November 1975

Final Report for Period September 1, 1973 — September 30, 1974

Prepared for

AIR FORCE ARMAMENT LABORATORY (DLMA)
EGLIN AIR FORCE BASE, FLORIDA 32542

NOTICES

When U. S. Government drawings specifications, or other data are used for any purpose other than a definitely related Government procurement operation, the Government thereby incurs no responsibility nor any obligation whatsoever, and the fact that the Government may have formulated, furnished, or in any way supplied the said drawings, specifications, or other data, is not to be regarded by implication or otherwise, or in any manner licensing the holder or any other person or corporation, or conveying any rights or permission to manufacture, use, or sell any patented invention that may in any way be related thereto.

Qualified users may obtain copies of this report from the Defense Documentation Center.

References to named commercial products in this report are not to be considered in any sense as an endorsement of the product by the United States Air Force or the Government.

This report has been reviewed by the Information Office (OI) and is releasable to the National Technical Information Service (NTIS). At NTIS, it will be available to the general public, including foreign nations.

APPROVAL STATEMENT

This technical report has been reviewed and is approved for publication.

FOR THE COMMANDER

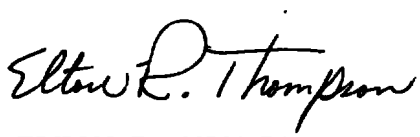

ELTON R. THOMPSON
Research & Development
Division
Directorate of Technology

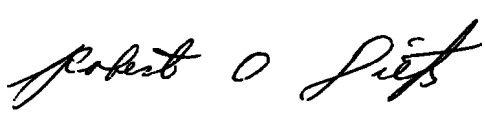

ROBERT O. DIETZ
Director of Technology

REPORT DOCUMENTATION PAGE		READ INSTRUCTIONS BEFORE COMPLETING FORM
1 REPORT NUMBER AEDC-TR-75-114 AFATL-TR-75-132	2 GOVT ACCESSION NO.	3 RECIPIENT'S CATALOG NUMBER
4 TITLE (and Subtitle) FLOW-FIELD STUDY ABOUT A HEMISPHERE-CYLINDER IN THE TRANSONIC AND LOW SUPERSONIC MACH NUMBER RANGE		5 TYPE OF REPORT & PERIOD COVERED Final Report, Sept 1, 1973 - Sept 30, 1974 6 PERFORMING ORG. REPORT NUMBER
7 AUTHOR(s) T. Hsieh, ARO, Inc.		8 CONTRACT OR GRANT NUMBER(s)
9 PERFORMING ORGANIZATION NAME AND ADDRESS Arnold Engineering Development Center (DY) Air Force Systems Command Arnold Air Force Station, TN 37389		10 PROGRAM ELEMENT, PROJECT, TASK AREA & WORK UNIT NUMBERS Program Element 62602F
11. CONTROLLING OFFICE NAME AND ADDRESS Air Force Armament Laboratory (AFATL/DLMA) Eglin Air Force Base, FL 32542		12 REPORT DATE November 1975 13. NUMBER OF PAGES 58
14 MONITORING AGENCY NAME & ADDRESS(if different from Controlling Office)		15 SECURITY CLASS. (of this report) UNCLASSIFIED 15a. DECLASSIFICATION/DOWNGRADING SCHEDULE N/A

16 DISTRIBUTION STATEMENT (of this Report)

Approved for public release; distribution unlimited.

17. DISTRIBUTION STATEMENT (of the abstract entered in Block 20, if different from Report)

18 SUPPLEMENTARY NOTES

Available in DDC.

19 KEY WORDS (Continue on reverse side if necessary and identify by block number)

hemispheres
aerodynamics
patterns
flow field
inviscid flow
transonic flow

20 ABSTRACT (Continue on reverse side if necessary and identify by block number)

A theoretical and experimental study has been conducted of a flow field about a hemisphere-cylinder at zero incidence in the transonic and low supersonic Mach number range (M_∞ = 0.7 to 2.0). For $M_\infty > 1$, the method used is a combination of the time-dependent solution for the hemispherical nose portion and the method-of-characteristics solution for the cylindrical body portion. Good agreement is found between theory and experiment

DD FORM 1 JAN 73 1473 EDITION OF 1 NOV 65 IS OBSOLETE

20. ABSTRACT (Continued)

for $M_\infty \geq 1.05$. The relaxation method has been used for Mach numbers from 0.7 to 1.3. This method gives good results for the pressure distribution over the complete body for Mach numbers from 0.95 to 1.3. Experimental results indicate a strong interaction of the shock and boundary layer for $M_\infty \approx 0.8$.

AFSC
Arnold AFS Tenn

PREFACE

The work presented herein was conducted by the Arnold Engineering Development Center (AEDC), Air Force Systems Command (AFSC), at the request of the Air Force Armament Laboratory (AFATL/DLMA) under Program Element 62602F. AFATL project monitor was Carroll B. Butler. The results of the research were obtained by ARO, Inc. (a subsidiary of Sverdrup & Parcel and Associates, Inc.), contract operator of AEDC, AFSC, Arnold Air Force Station, Tennessee, under ARO Project Numbers PF416, P34A-37A, and P33A-36A. The author of this technical report was T. Hsieh, ARO, Inc. The manuscript (ARO Control No. ARO-PWT-TR-75-35) was submitted for publication on March 24, 1975.

The author gratefully acknowledges the assistance of George Lewis and Wilbur Armstrong in the computation of results.

CONTENTS

ILLUSTRATIONS

TABLE

APPENDIX

1.0 INTRODUCTION

Many missiles have a spherically capped blunt nose. For missiles designed for high angle of attack, a blunt nose is sometimes preferred for the purpose of increasing stability. Therefore, a hemisphere-cylinder can be selected as a first step toward understanding the flow field over blunt-nose bodies. The reasons for selecting a hemisphere-cylinder are as follows: (1) a hemisphere-cylinder is simple in shape and can be used in the approximation of the flow field at the nose for spherically capped bodies, (2) a hemisphere nose retains its identity when the body is at an angle of attack, and (3) the hemisphere-cylinder itself has many engineering applications such as the well-known use of a flow probe or sensing device shape. In this report, the flow field about a hemisphere-cylinder at zero incidence is presented, and extension to an angle of attack will be reported separately. Understanding the flow field about a hemisphere-cylinder is particularly difficult for such a blunt shape when the free-stream Mach number is in the transonic and low supersonic flow range. As a first step toward understanding the flow phenomena about a hemisphere-cylinder, a fundamental and systematic study of the flow field about a hemisphere cylinder at zero incidence is presented in this report. Both theoretical and experimental results are presented for the Mach number range from 0.7 to 2.0.

As shown in Fig. 1, the flow past a hemisphere-cylinder may be described for two different cases, $M_\infty > 1$ and $M_\infty < 1$. For $M_\infty > 1$, the flow field influenced by introducing the

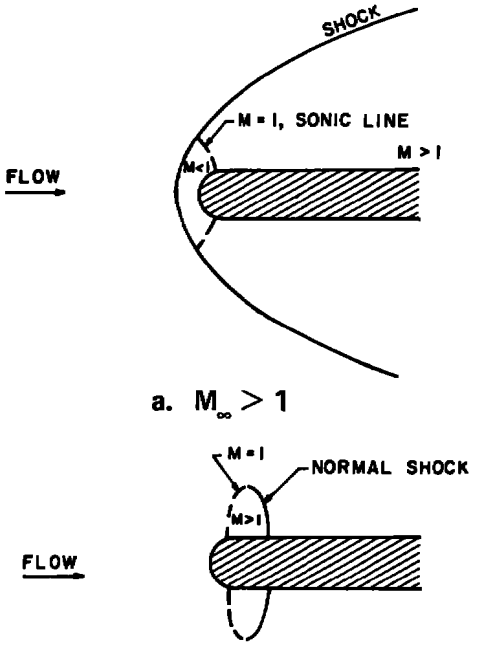

Figure 1. Description of flow field about hemisphere cylinder.

hemisphere-cylinder is restricted to the space enclosed by the bow shock and the body as shown in Fig. 1a. Behind the bow shock, the flow is divided by a sonic line into a subsonic region at the nose portion and a supersonic region downstream. On the other hand, for $M_\infty < 1$, the influence of the body covers all the flow space. As Mach number increases, two flow phenomena appear: a supersonic pocket and a normal shock extending from the body as shown in Fig. 1b. As $M_\infty \rightarrow 1$ subsonically, the supersonic region increases and the normal shock moves downstream. In principle, the bow shock moves upstream to infinity if $M_\infty = 1$ is approached supersonically, and the normal shock moves to infinity downstream (provided the cylinder is infinitely long) as $M_\infty = 1$ is approached subsonically. Consequently, there is no shock in the flow field at $M_\infty = 1$. However, in reality, the cylinder is finite, viscous effects exist, and shock systems will exist at $M_\infty = 1$. It is the purpose of this report to study how well these flow phenomena can be predicted by inviscid theory and to evaluate the accuracy of inviscid theory by comparison with experimental data.

Numerous theoretical studies of inviscid supersonic flow past blunt-nose bodies are reported in the literature (Refs. 1 through 6); however, the Mach numbers considered are generally greater than 2. Only a few studies (Refs. 2, 3, 5, and 6) for spherical nose shapes have been carried to Mach number 1.5 or 1.2, and the computations were limited to just a portion of the hemisphere. Among the various calculation techniques used, many investigators (Refs. 1 through 4) prefer the direct method of a time-dependent, finite-difference solution to the unsteady Euler's equations. The steady solution is obtained asymptotically as time advances. Even though this scheme has shown satisfactory results for a spherical nose for $M_\infty \geq 1.5$, the applicability of the method has not been investigated for $M_\infty < 1.5$. In this report, the numerical methods of Refs. 2 (modified and referred to as Code A) and 4* (referred to as Code B), based on the time-dependent finite-difference solution, were examined to check the validity of the solution at supersonic Mach numbers as low as 1.048 for the hemispherical nose portion. For the afterbody, the time-dependent scheme as described in Refs. 2 and 4 is not applicable at $M_\infty < 2$; therefore, the method of characteristics (Refs. 7 and 8) was utilized for the computation since the flow is supersonic everywhere downstream of the tangent points.

Not many calculations have been reported for blunt-nose bodies of revolution in subsonic, supercritical flow. To the author's knowledge, only two papers present solutions to this type of problem. In Ref. 9, a time-asymptotic, finite-difference method for solving the nonisentropic Euler's equations and exact boundary conditions for closed blunt bodies is presented; in Ref. 10 a finite-difference relaxation method is presented for numerical solution of the full potential equation and exact boundary conditions for general

*The computer program was made available to AEDC from Mr. Putz of Sandia Laboratory.

axisymmetrical bodies (blunt or pointed nose). The method of Ref. 10 is particularly convenient because it can treat bodies with an open end and is also applicable to a supersonic free stream. Therefore, it has been chosen for the hemisphere-cylinder study presented in this paper and is referred to as Code C. It is well known that in subsonic, supercritical flow, the interaction of the shock and boundary layer strongly changes the flow as predicted by the inviscid theory. The effects of the interaction for the hemisphere-cylinder studied will be discussed later in the presentation of results.

Experiments of supersonic flow past a spherical nose as related to the present study have been reported (Refs. 11 through 13). Data are available for the shock standoff distance and bow shock shape for M_∞ = 1.048 to 1.82. However, surface pressure data for a hemisphere-cylinder are available for $M_\infty \geq 1.42$ only. Shadowgraph and pressure data to evaluate the theoretical calculations were obtained at Mach numbers from 0.7 to 1.3 in the AEDC Propulsion Wind Tunnel (1T) for a 1-in.-diam, 10-in.-long hemisphere-cylinder.

2.0 THEORETICAL STUDY

Three different computational schemes have been employed in the present theoretical study of an inviscid, compressible flow past a hemisphere-cylinder at zero incidence for the Mach number range from 0.7 to 2.0. The reason is simply that there is not a single method that can be effectively applied to cover the entire flow range to be calculated.

2.1 TIME-DEPENDENT FINITE-DIFFERENCE SOLUTION TO THE UNSTEADY EULER'S EQUATIONS

This method is applied to the hemispherical nose portion as shown in Fig. 2a for $M_\infty > 1$. It is assumed that the sonic line is located ahead of the tangent point (this assumption holds for $M_\infty > 1.05$, approximately; see Appendix A), and so is the line of limiting characteristics. As a result, the flow downstream of the tangent point is supersonic everywhere and has no influence on the flow upstream of the tangent point. It is well known that the partial differential equations for the steady flow in this region are of mixed type (i.e., elliptic in the subsonic region and hyperbolic in the supersonic region) and are difficult to solve. One way to cope with the mixed elliptic-hyperbolic type of differential equations is to use the unsteady flow equations, which are always of the hyperbolic type. The steady solution is then obtained by advancing the time.

Among the many techniques reported for applying the time-dependent method to blunt-nose bodies, the direct method (Refs. 1 through 4) was chosen for this study. The computer programs (Refs. 2 and 4) with necessary modifications were used in the present calculation of the flow field about the nose portion. A brief description of the equations and numerical scheme used in obtaining solutions is given in the following paragraphs.

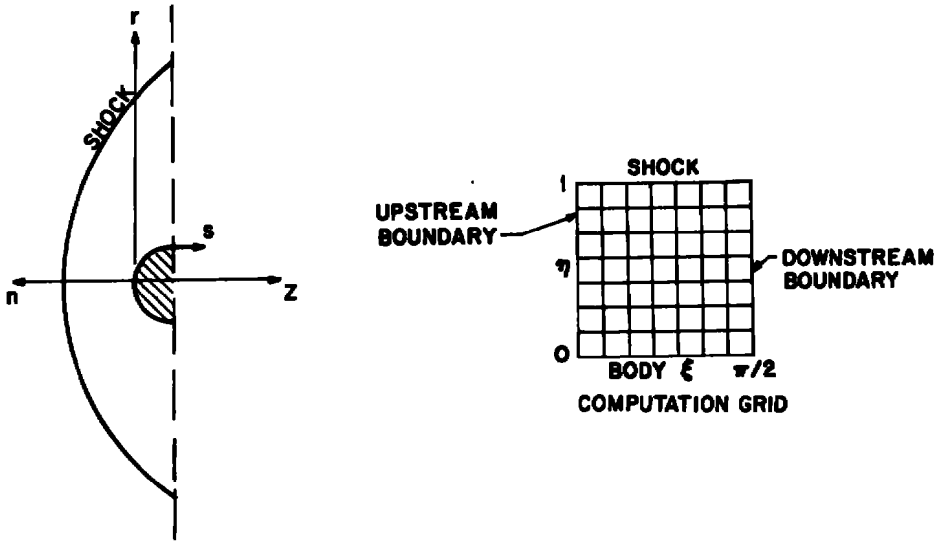

a. Time-dependent finite-difference method

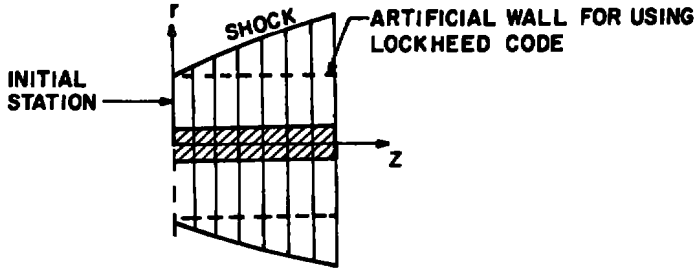

b. Method of characteristics

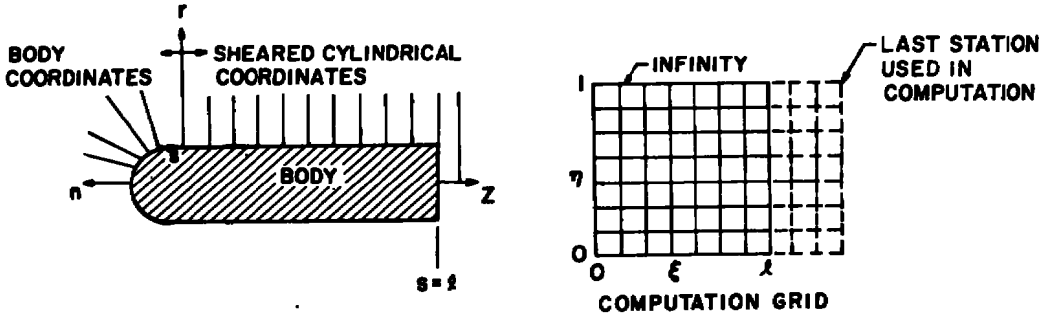

c. Relaxation method

Figure 2. Methods of calculation.

2.1.1 Differential Equations

The system of unsteady Euler equations written in a body-oriented coordinate system (s,n) are as follows:

$$\kappa r \frac{\partial \rho}{\partial t} + \frac{\partial (r\rho u)}{\partial s} + \kappa r \rho v = 0 \tag{1}$$

$$\kappa \frac{\partial u}{\partial t} + u \frac{\partial u}{\partial s} + \kappa v \frac{\partial u}{\partial n} + \frac{1}{\rho} \frac{\partial P}{\partial s} = Kuv \tag{2}$$

$$\kappa \frac{\partial v}{\partial t} + u \frac{\partial v}{\partial s} + \kappa v \frac{\partial v}{\partial n} + \frac{\kappa}{\rho} \frac{\partial P}{\partial n} = -K u^2 \tag{3}$$

$$\kappa \frac{\partial S}{\partial t} + u \frac{\partial S}{\partial s} - \kappa v \frac{\partial S}{\partial n} = 0 \tag{4}$$

$$P = \rho^{\gamma} e^{S/c_v} \tag{5}$$

It should be noted that Eq. (1) is singular at s = 0 and hence is replaced by

$$\kappa^2 \frac{\partial P}{\partial t} + 2\kappa \frac{\partial (\rho u)}{\partial s} + \frac{\partial (\kappa^2 \rho v)}{\partial n} = 0 \tag{6}$$

In Ref. 4, both spherical and cylindrical coordinate systems were used. In general, the system of equations is nondimensionalized and transformed into the rectangular calculation grid as shown in Fig. 2a.

2.1.2 Numerical Schemes

1. For the interior points in the computation grid, Ref. 2 approximates the spatial partial derivatives by a central difference and the time-partial derivatives by a forward difference. Stabilizing terms for artificial viscosity are added in such a way that the effects of the terms were made negligibly small (see Section 4.0). In Ref. 4, the interior points are computed by the implicit predictor-corrector scheme of Ref. 14.

2. The bow shock boundary conditions in both schemes are represented as a discontinuity, with the iteration scheme suggested in Ref. 1.

3. The body boundary conditions in Ref. 2 are represented by backward difference in the normal coordinates where v = 0 on the body surface (the other differences remain the same as for the interior points), whereas in Ref. 4 the body streamline conditions are satisfied by the same iteration scheme used in the shock boundary conditions.

In both Codes A and B the time interval that satisfies the stability requirement is automatically built in; therefore, one needs only to specify the nodal points and the number of advances in time. The steady condition is reached when the computed bow shock velocity, W_s, on the axis is sufficiently small (on the order of 10^{-4} to 10^{-5} of the free-stream sound speed).

2.2 METHOD OF CHARACTERISTICS

The flow field about the cylinder portion was computed by the method of characteristics. The General Applied Science Laboratories (GASL) three-dimensional method-of-characteristics code (Ref. 7) and the Lockheed axial symmetric internal flow code (Ref. 8) were used in the present study.

The characteristic equations in both codes were derived in detail in Refs. 8 and 15 and hence are not given here. The calculation proceeds from the initial station toward the downstream stations at each point as shown in Fig. 2b. It should be mentioned that in applying the method of Ref. 8, which was developed for nozzle flow, a cylindrical wall is artificially put in with a radius equal to the bow shock distance at the initial station, i.e., the tangent point (see Fig. 2b). As a result, as M_∞ increases, the bow shock moves closer and closer to the body, and the application of the Lockheed code deteriorates as calculation proceeds downstream. Therefore, in the present study, the Lockheed code was used only for $M_\infty < 1.3$ (where the artificial wall is sufficiently far from the body and has insignificant effects). The results obtained for the same initial data provide a comparison of the different computational schemes used by these two codes.

2.3 RELAXATION SOLUTION TO THE STEADY FULL POTENTIAL EQUATION

For $M_\infty < 1$, the partial differential equations are elliptic in nature; therefore, the entire flow field from the hemispherical cylinder to infinite space must be computed. When $M_\infty \leq 1$, the assumption of irrotational flow is approximately valid. Hence a solution to the steady full potential equation will describe the flow field. It is given as follows (Ref. 10):

$$\left(1 - \frac{u^2}{a^2}\right)\frac{1}{\kappa}\frac{\partial \psi}{\partial s}\left(\frac{1}{\kappa}\frac{\partial \psi}{\partial s}\right) - 2\frac{uv}{\kappa a^2}\frac{\partial^2 \psi}{\partial s \partial n} + \left(1 - \frac{v^2}{a^2}\right)\frac{\partial^2 \psi}{\partial n^2}$$

$$+ \left[\frac{K}{\kappa}\left(1 - \frac{u^2}{a^2}\right) + \frac{\cos\theta}{r}\right]\frac{\partial \psi}{\partial n} + 2\left(\frac{Kuv}{\kappa a^2} + \frac{\sin\theta}{r}\right)\frac{1}{\kappa}\frac{\partial \psi}{\partial s} = 0 \qquad (7)$$

The relation between ψ and the velocity components is

$$u = \cos\theta + \frac{1}{\kappa}\frac{\partial\psi}{\partial s} \tag{8a}$$

$$v = -\sin\theta + \frac{\partial\psi}{\partial n} \tag{8b}$$

Along the axis, Eq. (7) reduces to its limiting form,

$$\frac{2}{\kappa^2}\frac{\partial^2\psi}{\partial s^2} + \left(1 - \frac{v^2}{a^2}\right)\frac{\partial^2\psi}{\partial n^2} + 2\frac{K}{\kappa}\frac{\partial\psi}{\partial n} = 0 \tag{9}$$

The boundary conditions to be satisfied are

$$\psi \to 0 \text{ as } n \to \infty \tag{10a}$$

and

$$v = 0 \text{ or } \frac{\partial\psi}{\partial n} = \sin\theta \text{ on the body surface} \tag{10b}$$

As described in Ref. 10, sheared cylindrical coordinates are used for the afterbody. For the hemisphere-cylinder, Eqs. (7) through (10b) remain the same for the sheared cylindrical coordinates. As shown in Fig. 2c, by coordinate transformation the flow field was mapped into a rectangular computation plane (ξ-n), where the relaxation schemes were carried out. For $M_\infty \geq 1$, infinity is located about one body length behond the body end station, whereas for $M_\infty > 1$, the end station is used because the flow is supersonic there.

3.0 EXPERIMENTAL INVESTIGATION

Experiments were carried out for the purpose of evaluating the theoretical computations. As shown in Fig. 3, a hemisphere-cylinder 1 in. in diameter and 10 in. long was sting mounted in the AEDC Transonic Wind Tunnel (1T). A description of the wind tunnel may be found in Ref. 16. Pressure data were taken for Mach numbers from 0.7 to 1.3. Shadowgraphs were taken for M_∞ = 0.8, 0.9, 0.95, 1.0, 1.05, 1.1, 1.2, and 1.3. The shock standoff distance and shock shape for $M_\infty > 1$ and the normal shock on the cylinder for $M_\infty < 1$ were obtained from the shadowgraphs.

In addition to the experimental data described above, the experimental results of Refs. 11 through 13 were also used to evaluate the theoretical results.

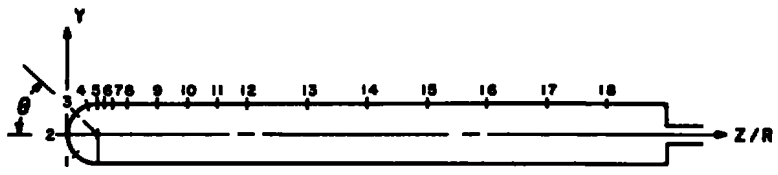

PRESSURE ORIFICE NO.	1	2	3	4	5	6	7	8	9	10	11	12	13	14	15	16	17	18
LOCATION, Z/R	.271	0	.271	.708	1.0	1.25	1.5	2.0	3.0	4.0	5.0	6.0	8.0	10.0	12.0	14.0	16.0	18.0
θ	-45°	0	45°	75°	90°													

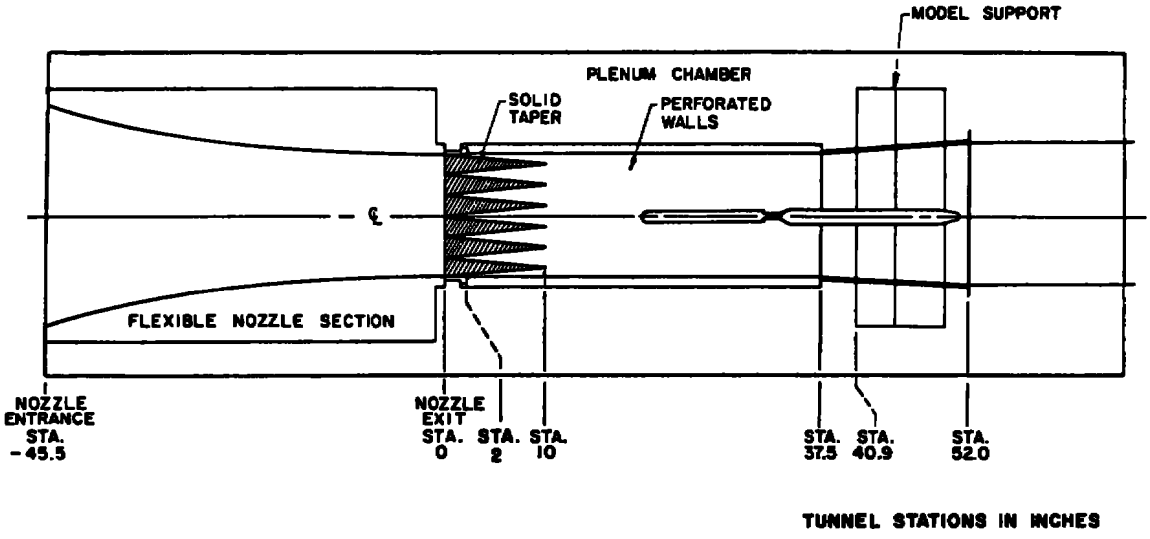

Figure 3. Model and testing setup.

4.0 DISCUSSION OF RESULTS

In the following paragraphs, the theoretical results are compared with other theoretical calculations reported in the literature and with experimental data available. The validity of each method of calculation is discussed and evaluated. To facilitate presentation, results are described in two parts, $M_\infty > 1$ and $M_\infty \leq 1$.

4.1 LOW SUPERSONIC MACH NUMBER RANGE, $2 > M_\infty > 1$

4.1.1 Accuracy of Computation and Computer Time

For $M_\infty > 1$, the flow about the hemispherical nose portion was calculated mainly by Code A. Computation with Code B was also made for comparison. Since stabilizing terms are added in Code A and Code A results were used as initial values for the continuing computation of the cylinder portion by the method of characteristics, the accuracy of Code A must be evaluated first. The accuracy is judged by two quantities, the stagnation

pressure and the total enthalpy. For all cases computed, the stagnation pressure was off by no more than 1.5 percent and the deviation of total enthalpy was no more than 1 percent; this is considered to be satisfactory. The values of pressure, P, and the u and v components at the end station of the hemispherical nose are tabulated in Appendix A. These values were used as the intial conditions in the computer program for the method of characteristics.

For the IBM 370-155 computer, with which all the computations were performed, the computation time required about 3×10^{-3} sec per nodal point per time step. As Mach number decreases, the nodal points and the time steps required for good results increase rapidly. The approach to steady state is judged by the ratio of the shock speed, W_s, to the free-stream sound speed. A list of the mesh size, time steps, and shock speed for some typical Mach number values is given in Table 1.

Table 1. Hemisphere Nose Computational Data

M_∞	Nodal Points	Time Steps	Shock Speed, $W_s/\sqrt{p_\infty/\rho_\infty}$	
			At Axis	At Shoulder
1.82	12 x 12	1,610	0.1×10^{-4}	0.7×10^{-3}
1.60	12 x 12	2,531	0.1×10^{-4}	0.8×10^{-3}
1.50	13 x 13	3,500	0.7×10^{-5}	0.6×10^{-3}
1.42	16 x 16	4,451	0.1×10^{-4}	0.9×10^{-3}
1.30	16 x 16	8,000	0.2×10^{-4}	0.1×10^{-2}
1.20	24 x 24	12,000	0.7×10^{-4}	0.6×10^{-2}
1.10	30 x 30	22,000	0.4×10^{-3}	0.3×10^{-1}
1.05	30 x 30	30,000*	0.14×10^{-2}	0.6×10^{-1}

*Discontinued because of too-slow convergence.

For example, at $M_\infty = 1.5$, a mesh of 13 x 13 and 3500 time steps gives good results; however, for $M_\infty = 1.2$, one needs 24 x 24 mesh and 12,000 time steps. It is important to point out that the surface pressure approaches steady state in much fewer time steps than does the shock standoff distance. For example, at $M_\infty = 1.1$ with 2000 time steps the pressure reaches its final value within 1 percent at the nosetip and 6 percent at the tangent point, and with 4000 time steps the corresponding values reduce to 0.5 and 4 percent, respectively. In contrast, the shock standoff distance at the nose is 34 and 14 percent of the steady-state value with time steps of 2000 and 4000, respectively. Figure 4 shows the asymptotical approach to the steady-state shock standoff distance for $M_\infty = 1.2$, 1.1, and 1.05. It should be noted that for $M_\infty = 1.05$, the computation stops at 30,000 time steps because of too slow a convergence, and the steady-state Δ/R value was obtained by extrapolation.

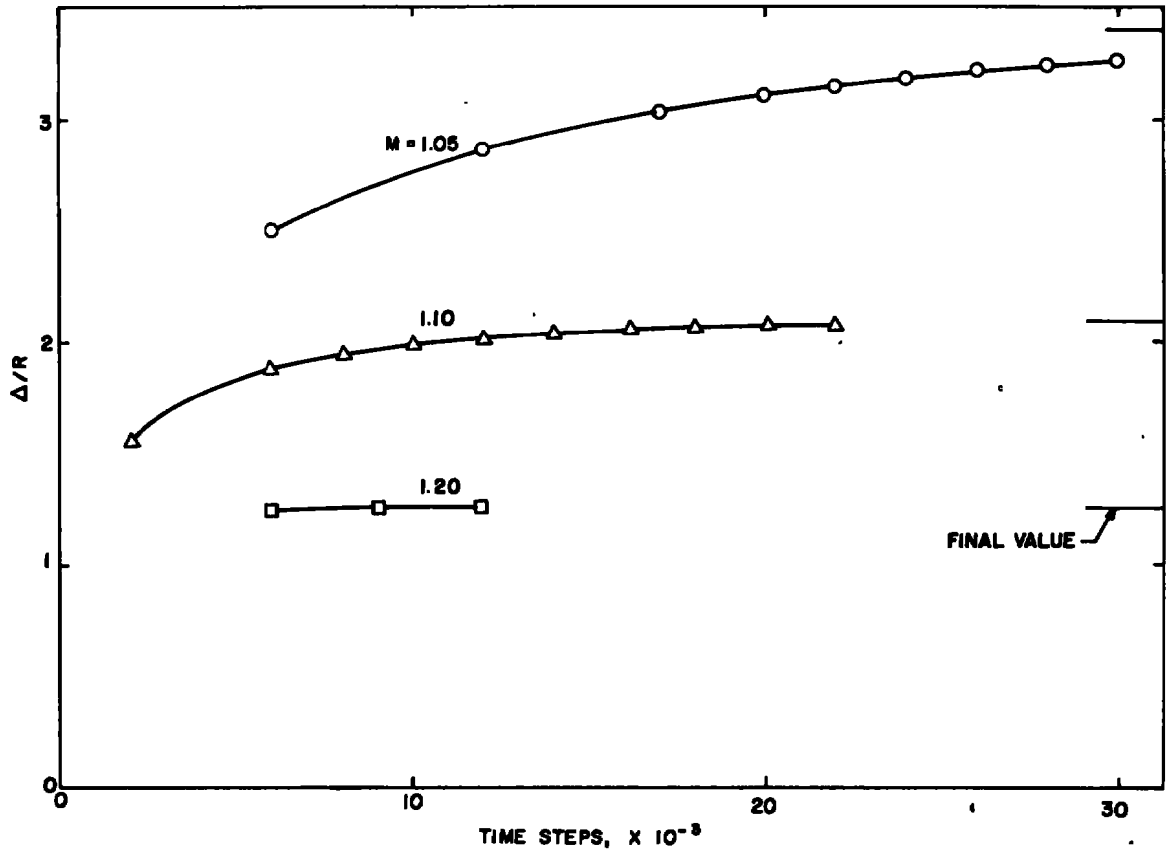

Figure 4. Shock standoff distance versus time steps.

4.1.2 Shock Standoff Distance

In Fig. 5, the bow shock standoff distance Δ/R is plotted as a function of free-stream Mach number, $M_\infty > 1$. The curves and the solid symbols are from various theoretical results, and the open symbols are experimental data from various sources. It should be noted that the experimental data (Refs. 11 and 13) are for spheres. Since the flow becomes supersonic before it reaches the tangent point for all data presented in Fig. 3 (see Appendix A), the standoff distance and the bow shock shape for the hemispherical nose should be valid for comparison with the sphere. (Note that the influence of limiting characteristics at $1.0 < M_\infty < 1.1$ remains to be investigated.) Two values of $\gamma = 1.4$ and 1.13 are shown in the figure to compare with the available data. The agreement for different theoretical predictions is excellent except for Ref. 6, which predicts a smaller standoff distance as the Mach number decreases, and Code C (Ref. 10), which consistently predicts a larger value. The comparison of the present theoretical results with experiments is also satisfactory except in the very low Mach number range, $1.05 < M_\infty < 1.13$, where the experimental data (Ref. 11) are lower than the theory. The AEDC experimental data for

air, γ = 1.4, are consistently less. This remains to be investigated.* Generally speaking, the shock standoff distance for a hemisphere-cylinder can be predicted by inviscid theory at low supersonic Mach numbers.

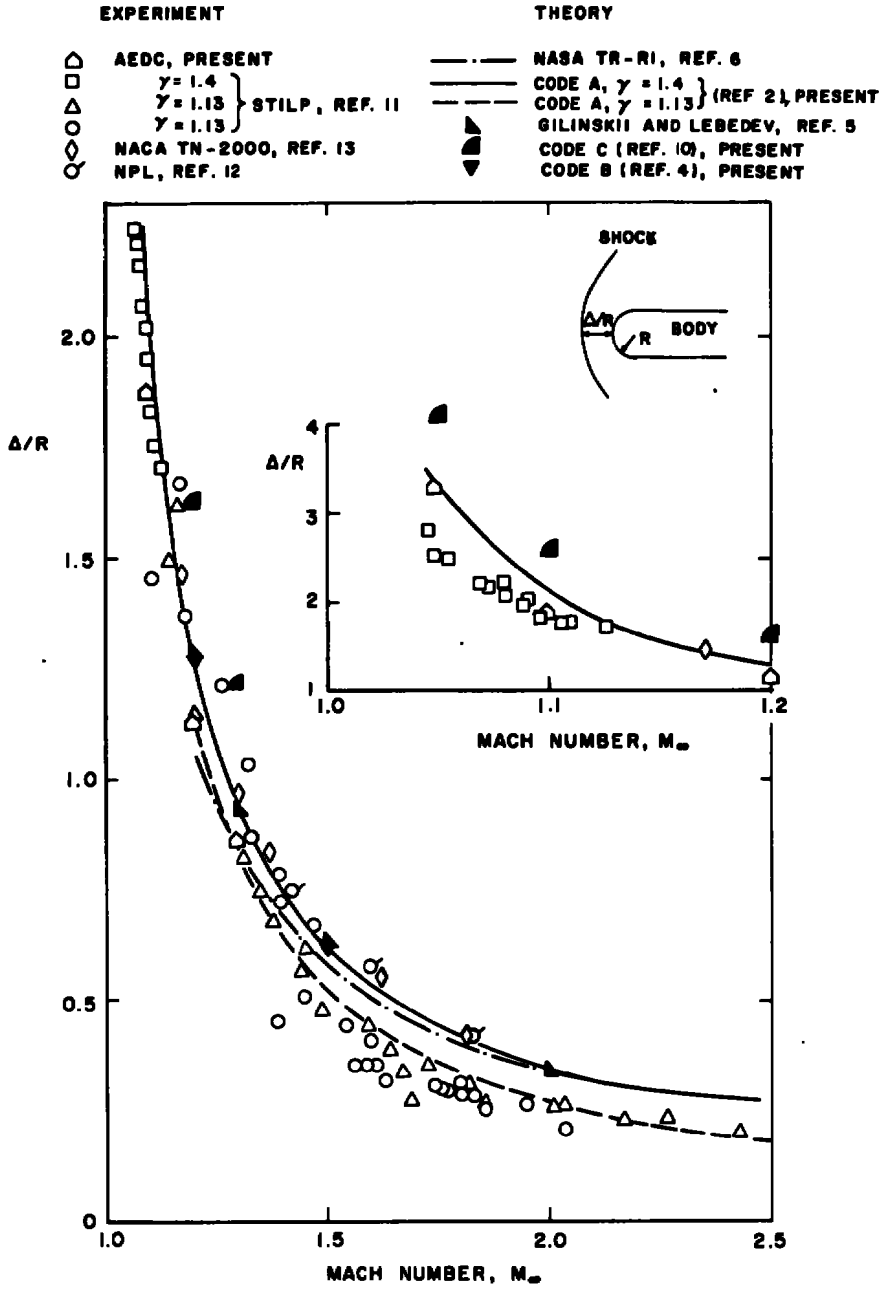

Figure 5. Comparison of shock standoff distance between calculation and experiment.

*See Appendix B.

4.1.3 Shock Characteristics

Different methods of predicting the bow shock are shown in Fig. 6. The agreement is satisfactory. Reference 6 gives a smaller shock layer than the other methods as Mach number decreases. Code A predicts a shock shape with less curvature than Code B for all cases studied. Figure 7 shows a comparison between the theoretical calculation and available experimental data. The agreement between the present calculations and the data

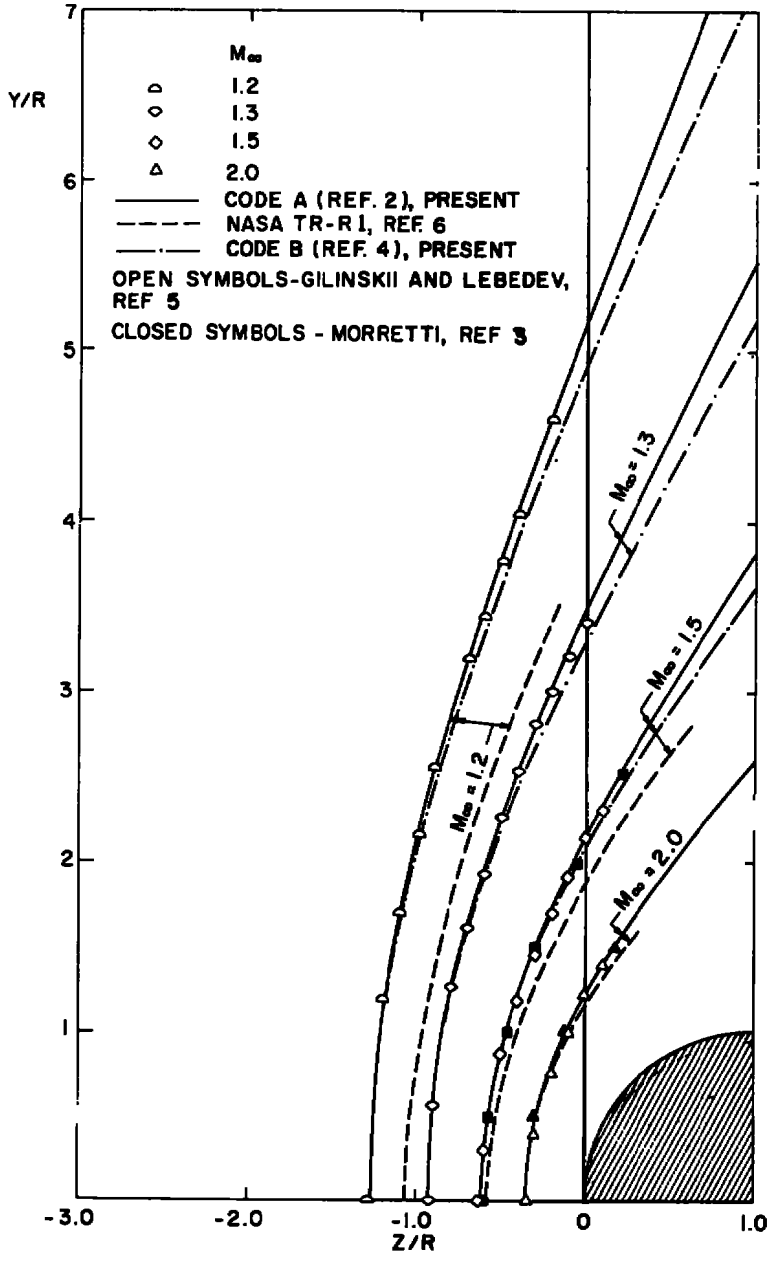

Figure 6. Comparison of theoretical shock position.

of Ref. 9 is surprisingly good to a Mach number as low as $M_\infty = 1.17$. Again the AEDC data show a thinner shock layer (see Fig. B-3 for new data).

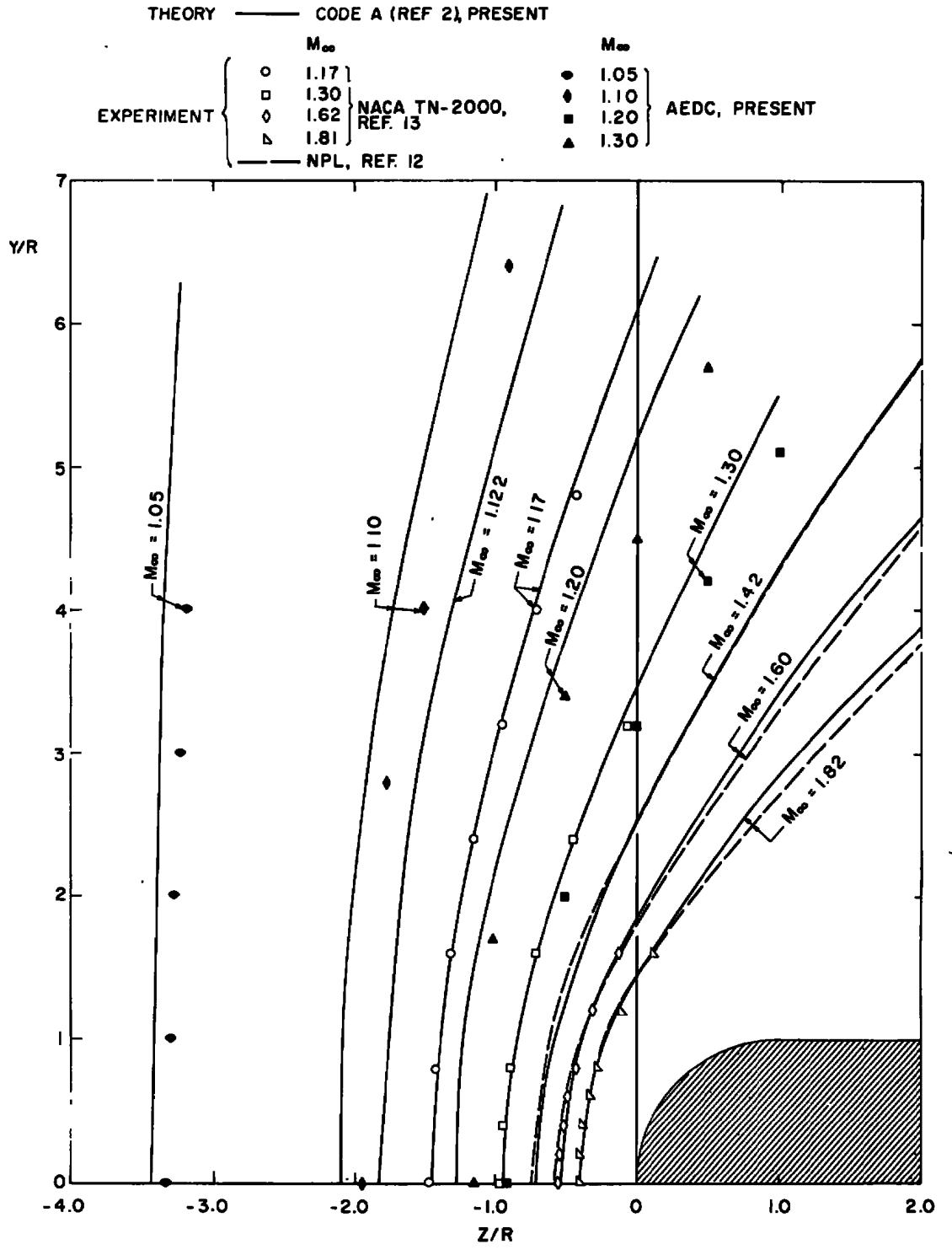

Figure 7. Comparison of theoretical shock position with experiment, $\gamma = 1.4$.

4.1.4 Sonic Lines

The sonic lines calculated by different methods are compared in Fig. 8. Calculations from Codes A and B compare well with each other and with results of Refs. 3 and 5 for $M_\infty \geq 1.5$. For $M_\infty \leq 1.3$, the sonic line predicted by each method starts to deviate

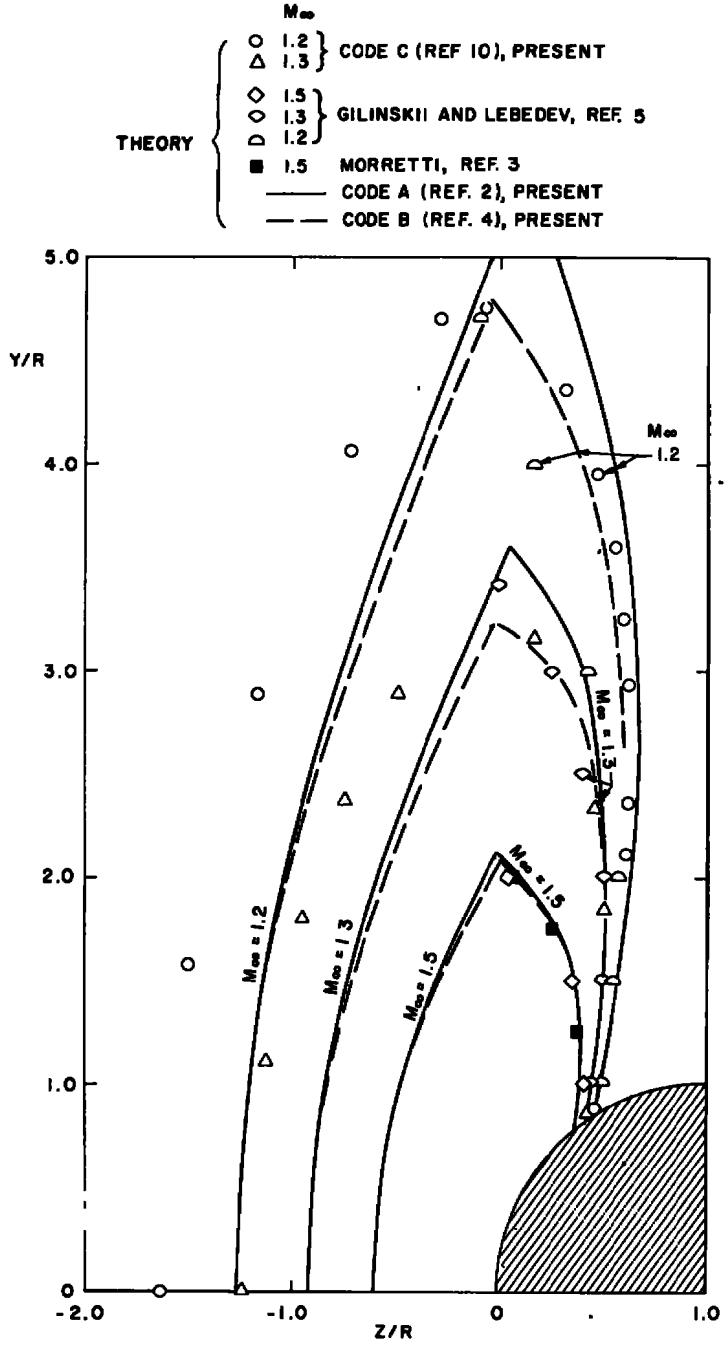

Figure 8. Comparison of sonic lines.

as the distance away from the body increases. The relaxation method predicts a too-large subsonic region with the bow shock front too far away from the nose. However, in the region close to the body, the sonic lines predicted by each method converge. At M_∞ = 1.2, Code B gives irregular numbers for all the flow variables in the region close to the body (see Fig. 9 also). Nevertheless, the shock shapes are still good, and the part of the sonic line close to the shock can still be sketched as shown in Fig. 8. Significant differences in the sonic line location are shown between the present calculation and Ref. 5 for M_∞ = 1.2. At the present time, no experimental data are available for comparison of the sonic line location and hence no evaluation can be made of the prediction methods.

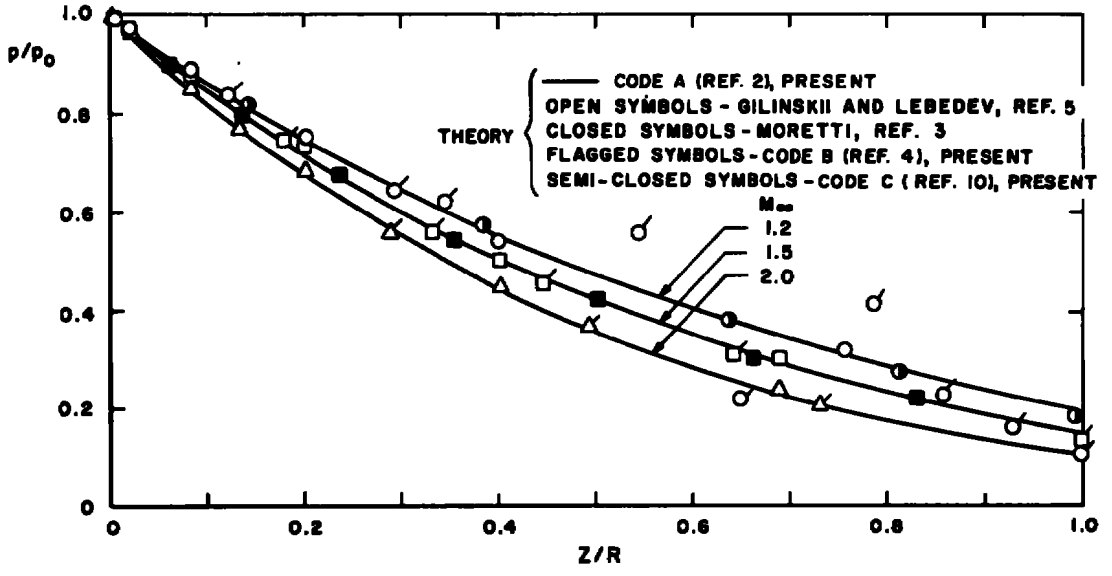

Figure 9. Comparison of theoretical pressure over the hemisphere nose.

4.1.5 Surface Pressure

Figure 9 shows the calculated pressure distribution on the hemisphere part from various sources. The agreement is quite satisfactory. As described previously, at M_∞ = 1.2 the results from Code B start to oscillate about $Z/R > 0.4$ (the same mesh number was used as the Code A, and it was also found that increasing the nodal points would not help to improve the result), and it will not run for $M_\infty < 1.2$. Thus, for $M_\infty \leq 1.2$, Code A is the only satisfactory code.

The favorable comparison of Fig. 9 for the nose portion gives some confidence to use the data obtained from Code A at the end station of the hemispherical nose to start the computation of the flow about the cylindrical portion by the method of characteristics. The initial data of P,u,v used in the present calculations are shown in Fig. 10 for $(Y-1)/R \leq 3.8$. A test run was carried out for M_∞ = 1.2 with both the GASL code and the Lockheed

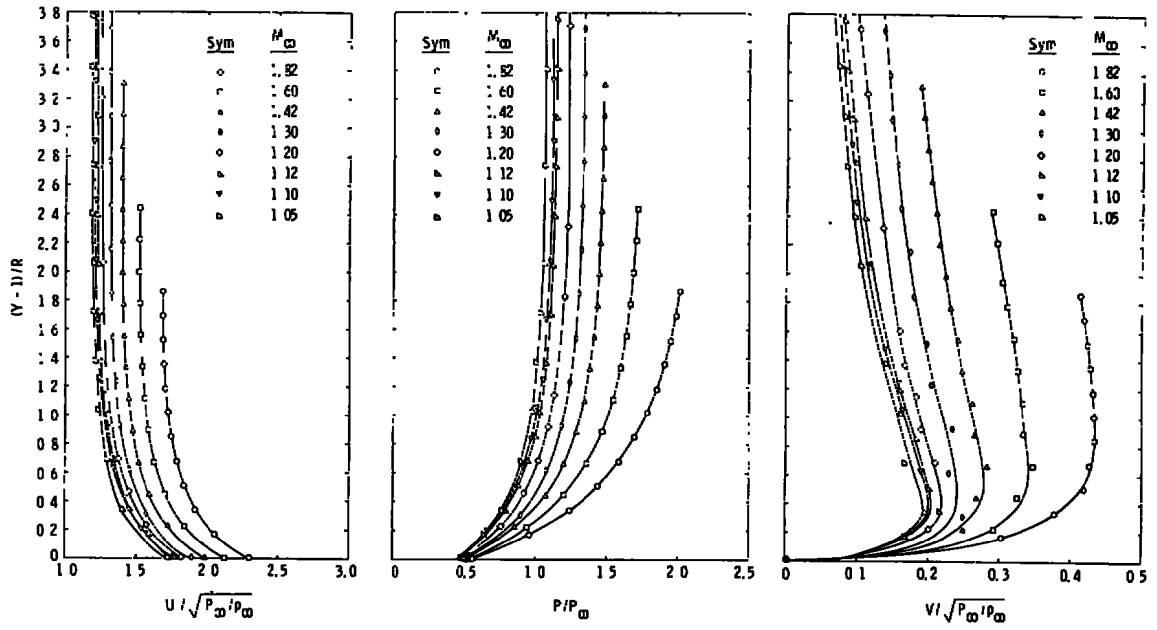

Figure 10. Initial data for MOC calculation.

code with the same initial data. It was found that the GASL code requires twice the initial nodal points (initial data were linearly interpolated for the additional nodal points) as the Lockheed code to obtain the same accuracy as shown in Fig. 11. On the other hand, the Lockheed code is unsatisfactory for the downstream surface pressure when $M_\infty > 1.3$ (see Section 2.0 for explanation). For the low supersonic Mach numbers, the GASL code was used for $M_\infty \geq 1.1$ (it would not run for $M_\infty = 1.05$), and the Lockheed code was used for $M_\infty = 1.05$ to 1.3. The overlapping Mach number range ($M_\infty = 1.1$, 1.2, and 1.3) provided a comparison of results. Figure 11 shows that the comparison is satisfactory. In Fig. 12, the calculated surface pressures are compared with experimental data. It is seen that for all cases calculated, the time-dependent method plus the method of characteristics gives very good agreement with experiment. It should be noted that for $M_\infty = 1.05$ the calculation broke down in the cylinder portion at $Z/R = 2.5$ because of too-low Mach number. Calculations were also carried out for Mach numbers up to 1.42 by using the relaxation method of Ref. 10 (with IBM 370-155, a complete case using a mesh halving scheme of 25 x 25, 49 x 49, and 97 x 97 requires approximately 35 minutes of computer time). Surprisingly enough, the agreement between the relaxation method and the experiments is good up to $M_\infty = 1.3$, particularly for the minimum pressure at the tangent point. For $M_\infty = 1.42$, the pressure predicted by the relaxation method is not satisfactory and hence is not shown.

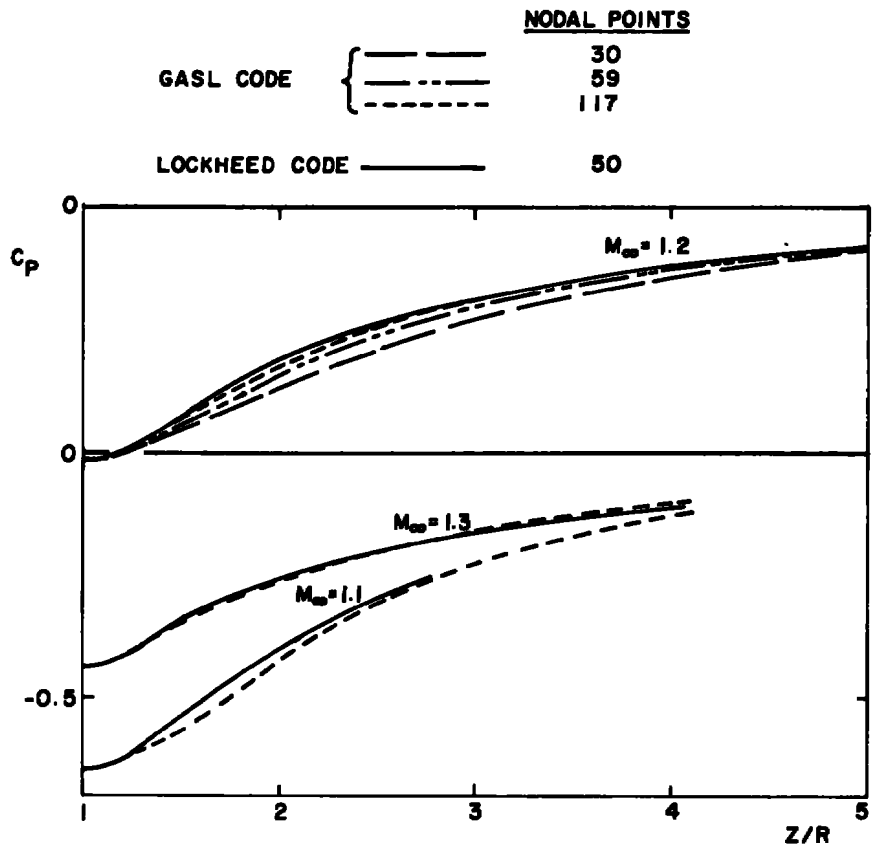

Figure 11. Comparison of MOC calculations.

4.1.6 Oblique Shock

The shadowgraphs (Fig. 13) show that systems of weak oblique shocks exist downstream of the tangent point; these indicate an overexpansion of the flow for most Mach numbers. The major or first oblique shocks each have nearly the same shock angle (i.e., about 40 to 50 deg for the range of Mach number shown). It is interesting to note that in plotting the characteristic lines obtained from the Lockheed code, a coalescing of the characteristic lines indeed indicates the appearance of an oblique shock as shown in Fig. 14 for M_∞ = 1.2. If the results of Fig. 13 are compared with those of Fig. 14 for M_∞ = 1.2, the slope and location of the major oblique shock are roughly predicted by inviscid theory.

4.1.7 Flow Characteristics in the Shock Layer

To describe the entire flow within the shock layer, a mapping of the pressure and Mach number distribution obtained by Code A and GASL code for M_∞ = 1.1, 1.122, 1.2, 1.3, and 1.42 is shown in Figs. 15 and 16, respectively.

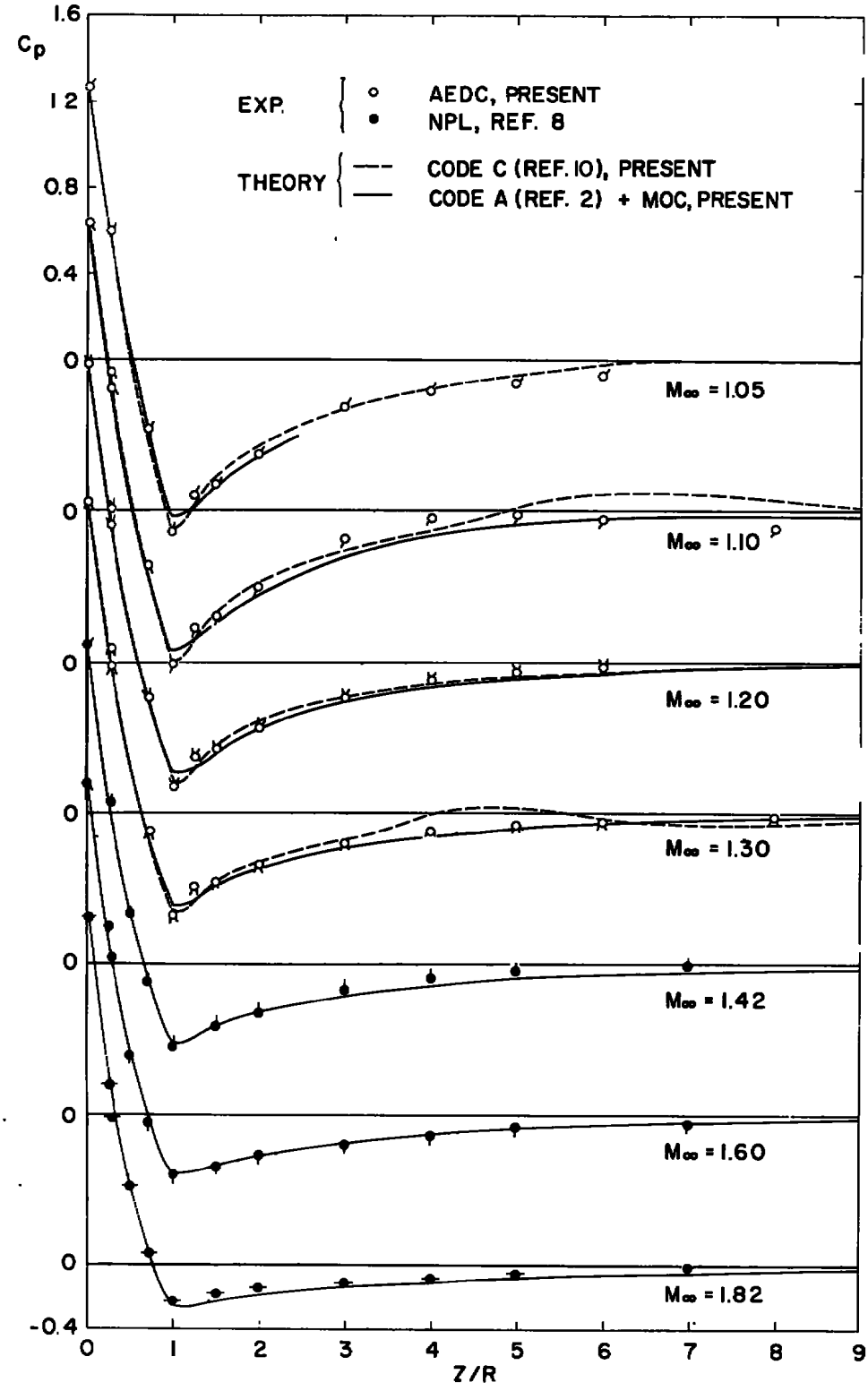

Figure 12. Comparison of the theoretical pressure distribution with experiments.

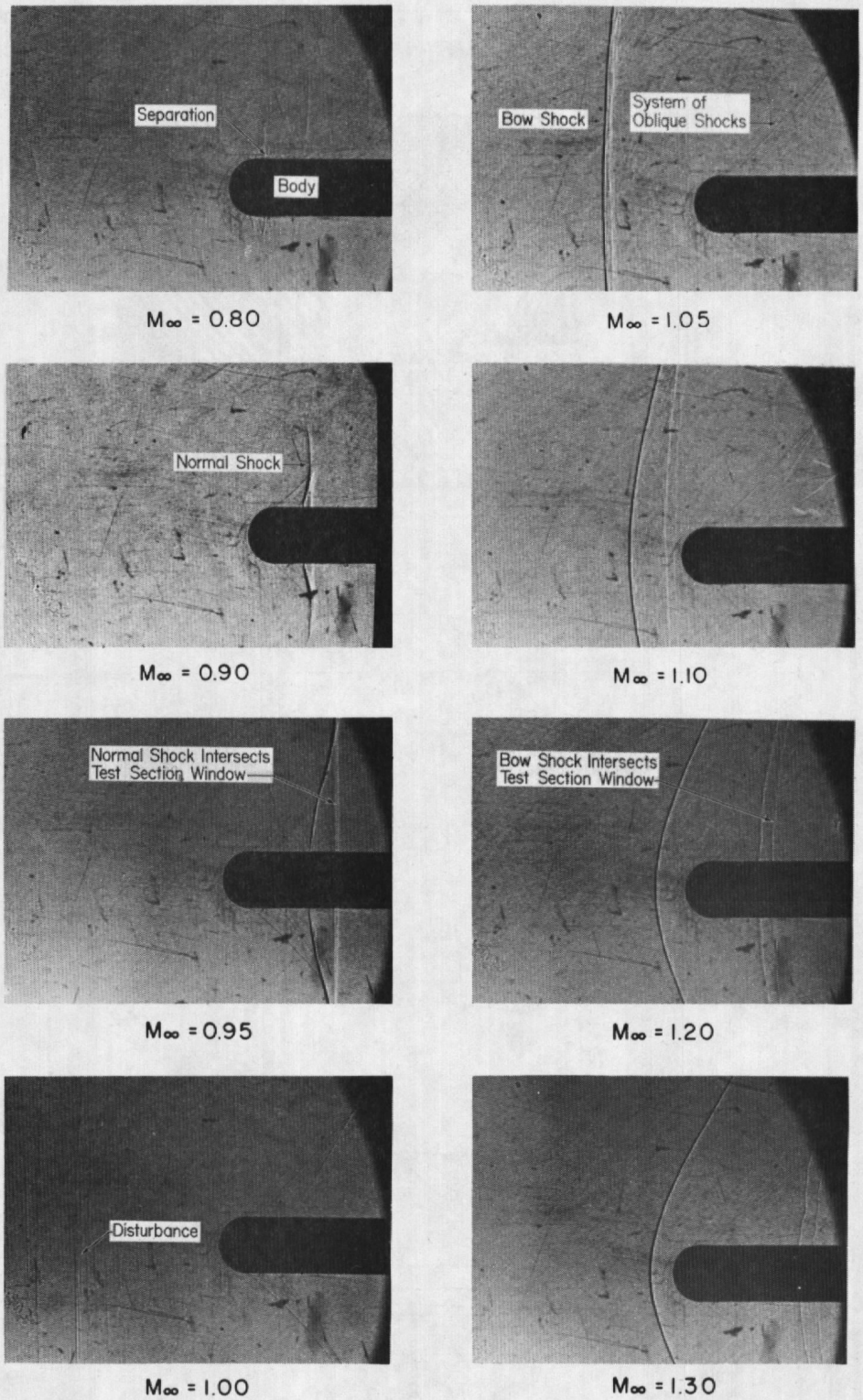

Figure 13. Shadowgraphs of flow past hemisphere-cylinder.

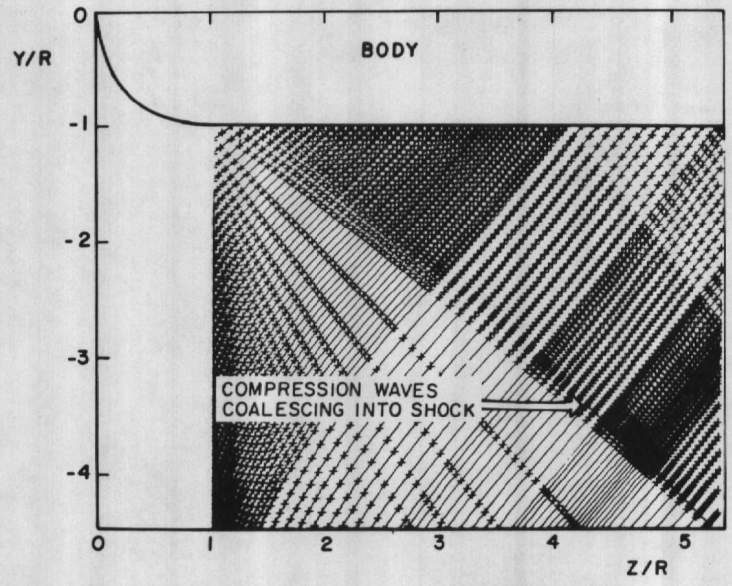

Figure 14. Plot of characteristic lines for M_∞ = 1.2.

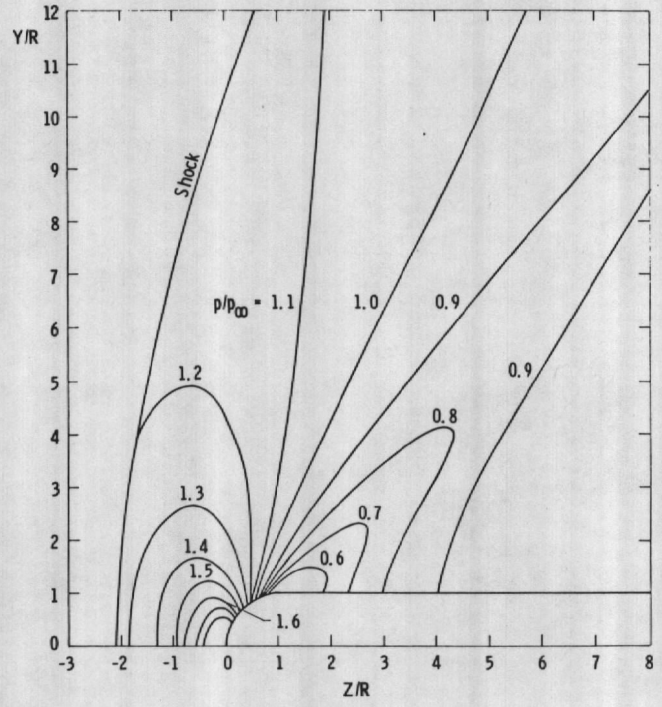

a. M_∞ = 1.1

Figure 15. Mapping of pressure distribution in the shock layer.

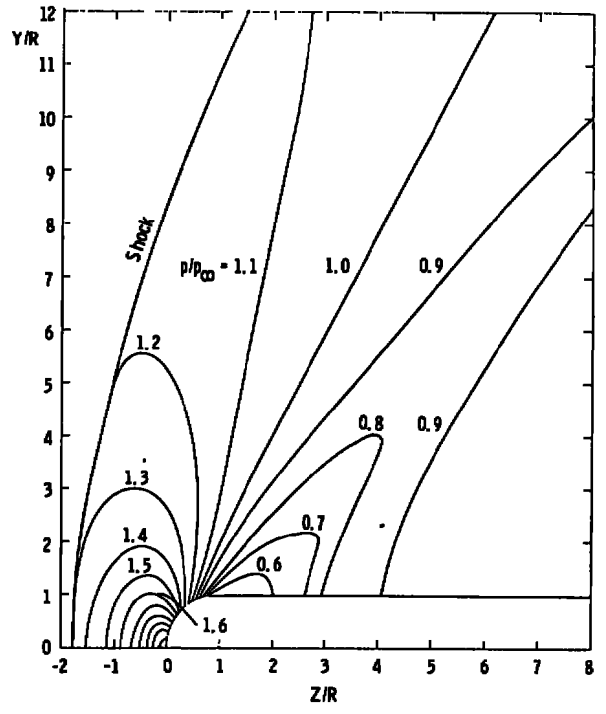

b. $M_\infty = 1.122$

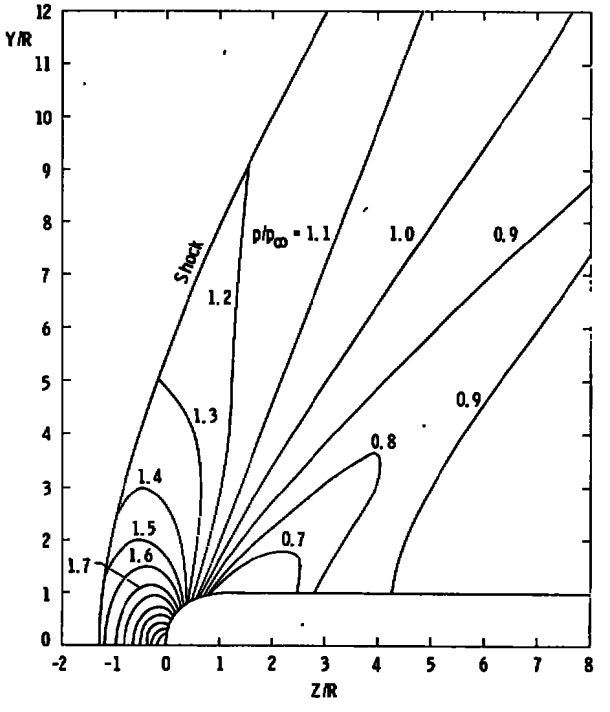

c. $M_\infty = 1.2$

Figure 15. Continued.

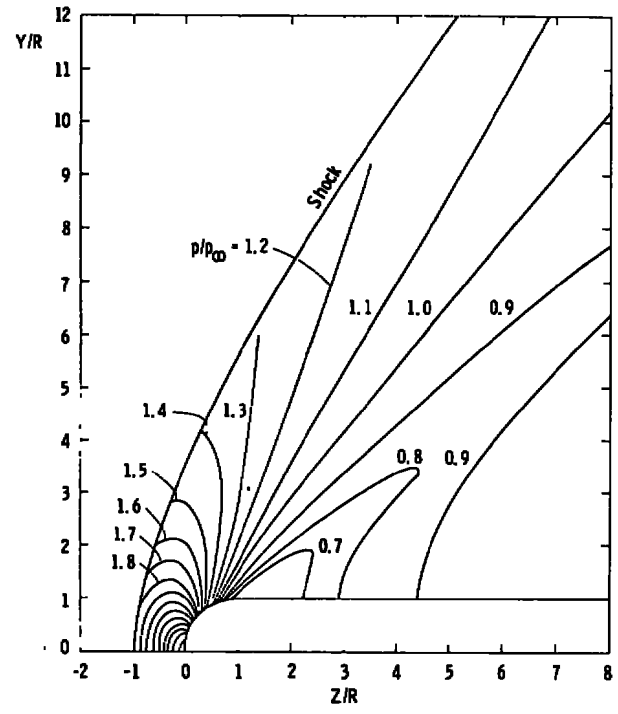

d. $M_\infty = 1.3$

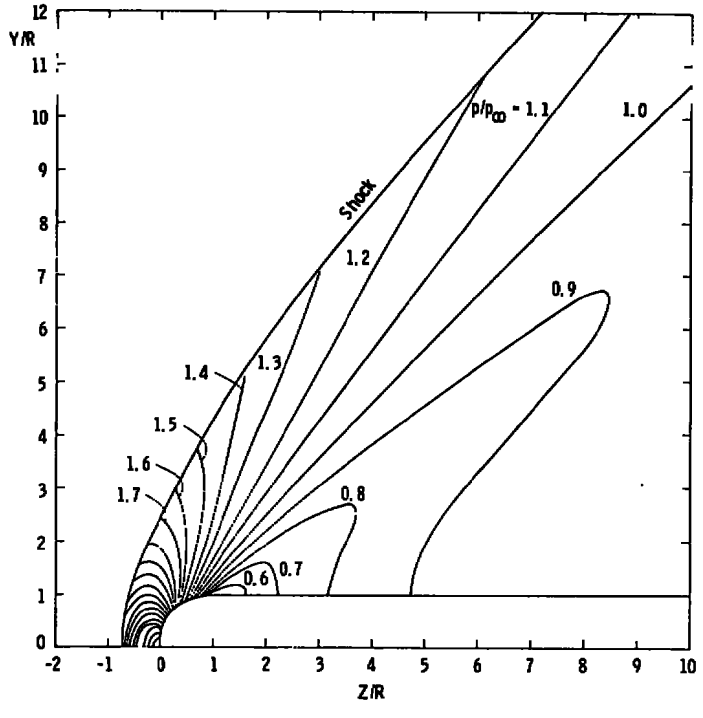

e. $M_\infty = 1.42$

Figure 15. Concluded.

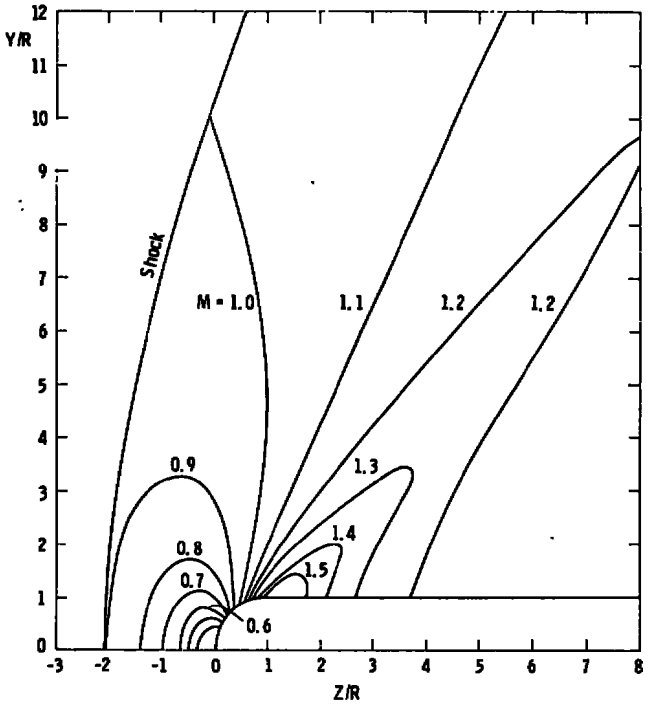

a. $M_\infty = 1.1$

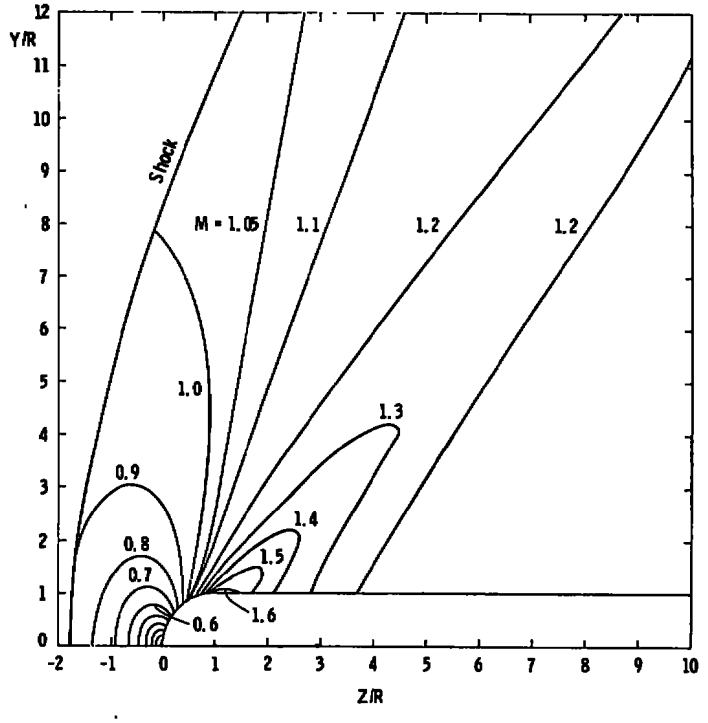

b. $M_\infty = 1.122$

Figure 16. Mapping of Mach number distribution in the shock layer.

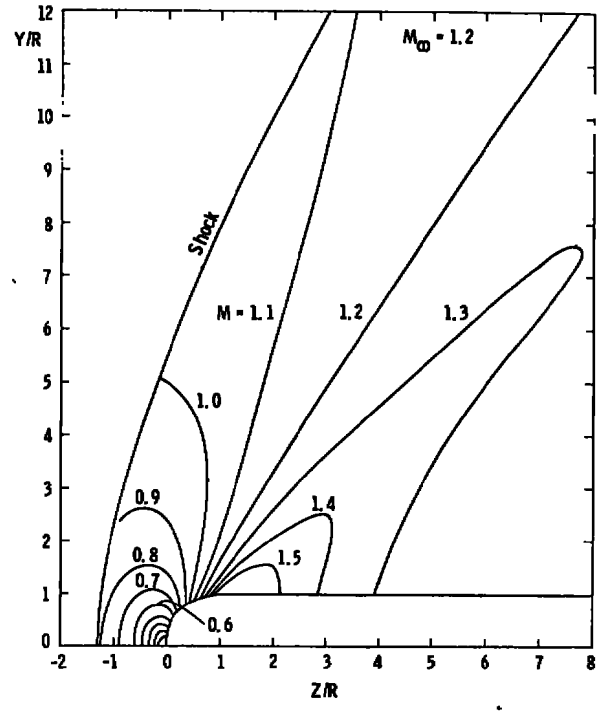

c. M_∞ = 1.2

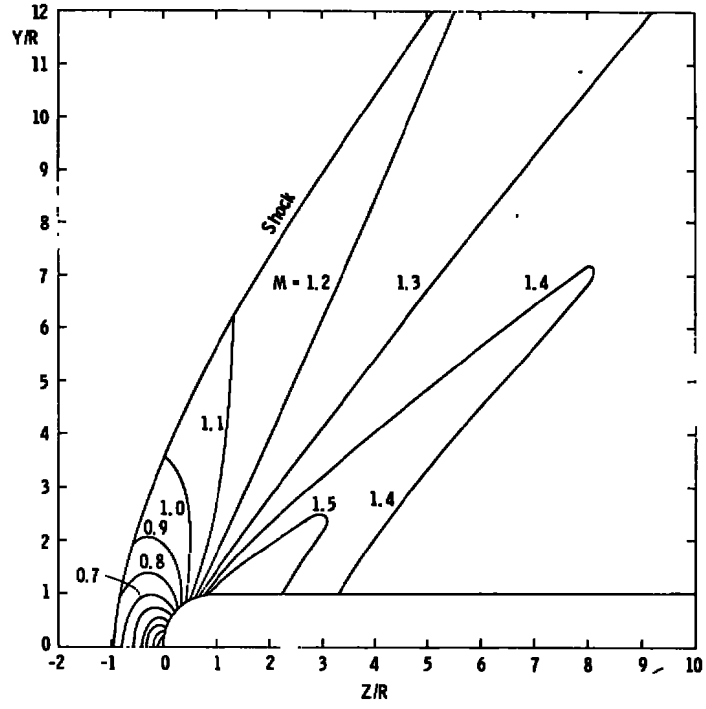

d. M_∞ = 1.3

Figure 16. Continued.

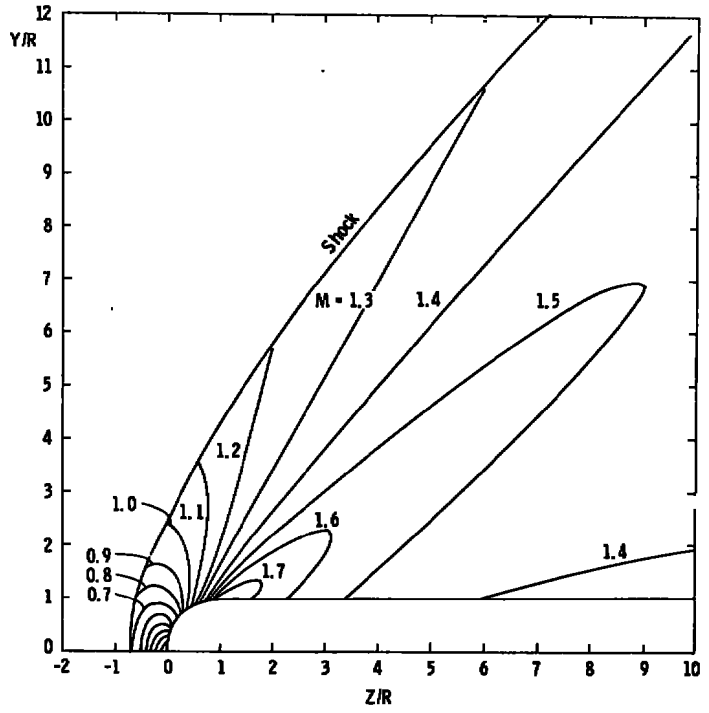

e. $M_\infty = 1.42$

Figure 16. Concluded.

4.2 TRANSONIC MACH NUMBER RANGE, $0.7 < M_\infty \leq 1$

4.2.1 Supersonic Pocket and Normal Shock

In Fig. 17, a comparison is presented of the location of the supersonic pocket and shock calculated by the relaxation method of Ref. 10 (note that the method of Ref. 10 does not use the conservative differencing with a "shock point" operator as does Ref. 17) and obtained from the shadowgraphs of Fig. 13. It is seen that the shape of the shock for the cases shown is predicted correctly, but the location is shifted. The experimental results show the shock occurred some distance downstream.

4.2.2 Surface Pressure

In Fig. 18 the surface pressure calculated by the relaxation method is compared with the experimental data for $M_\infty \leq 1$. It is seen that the theory satisfactorily predicts the pressure distribution up to the location where the shock seems to appear. For $M_\infty = 0.8$ there is stronger disagreement in the theoretical and experimental pressure distribution. The corresponding shadowgraph given in Fig. 10 does indicate a pronounced boundary-layer separatation for $M_\infty = 0.8$. The same phenomenon occurs to a lesser degree at other Mach

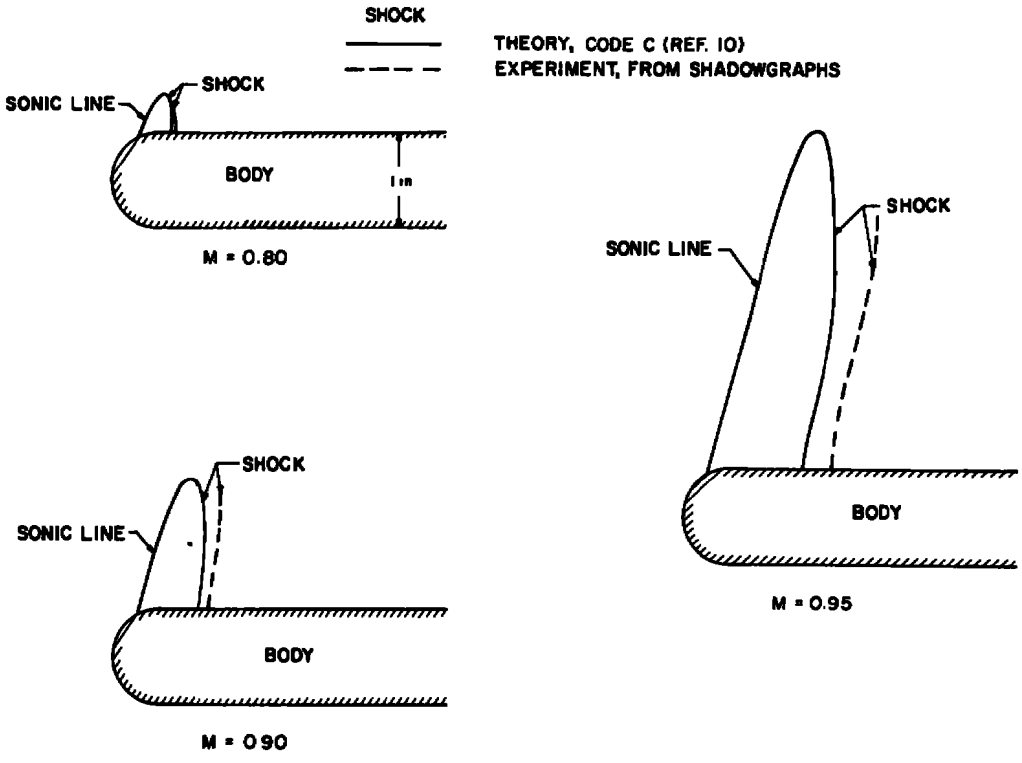

Figure 17. Comparison of supersonic pocket and normal shock.

numbers. Therefore, it is assumed that the difference in experimental and theoretical pressure distribution for $0.7 < M_\infty < 1.0$ is caused by the interaction of the shock and the boundary layer.

4.2.3 Sonic Flow, $M_\infty = 1$

Sonic flow presents a fascinating case in both theory and experiment. One is pleased to see the good agreement between prediction and data in the surface pressure. It would be interesting to point out that the disturbances (not shocks) upstream of the cylinder as shown in Fig. 13 for $M_\infty = 1$ have the counterpart in the numerical computation (Fig. 19). The theory indeed predicts a supersonic pocket which extends to infinity. Also, the sonic line moves beyond the plane of the shoulder. With finite length of the cylinder, the shock is located near the end of the cylinder as predicted by the theory. Unfortunately, the shadowgraph for $M_\infty = 1$ does not cover the tail end of the cylinder to offer a comparison.

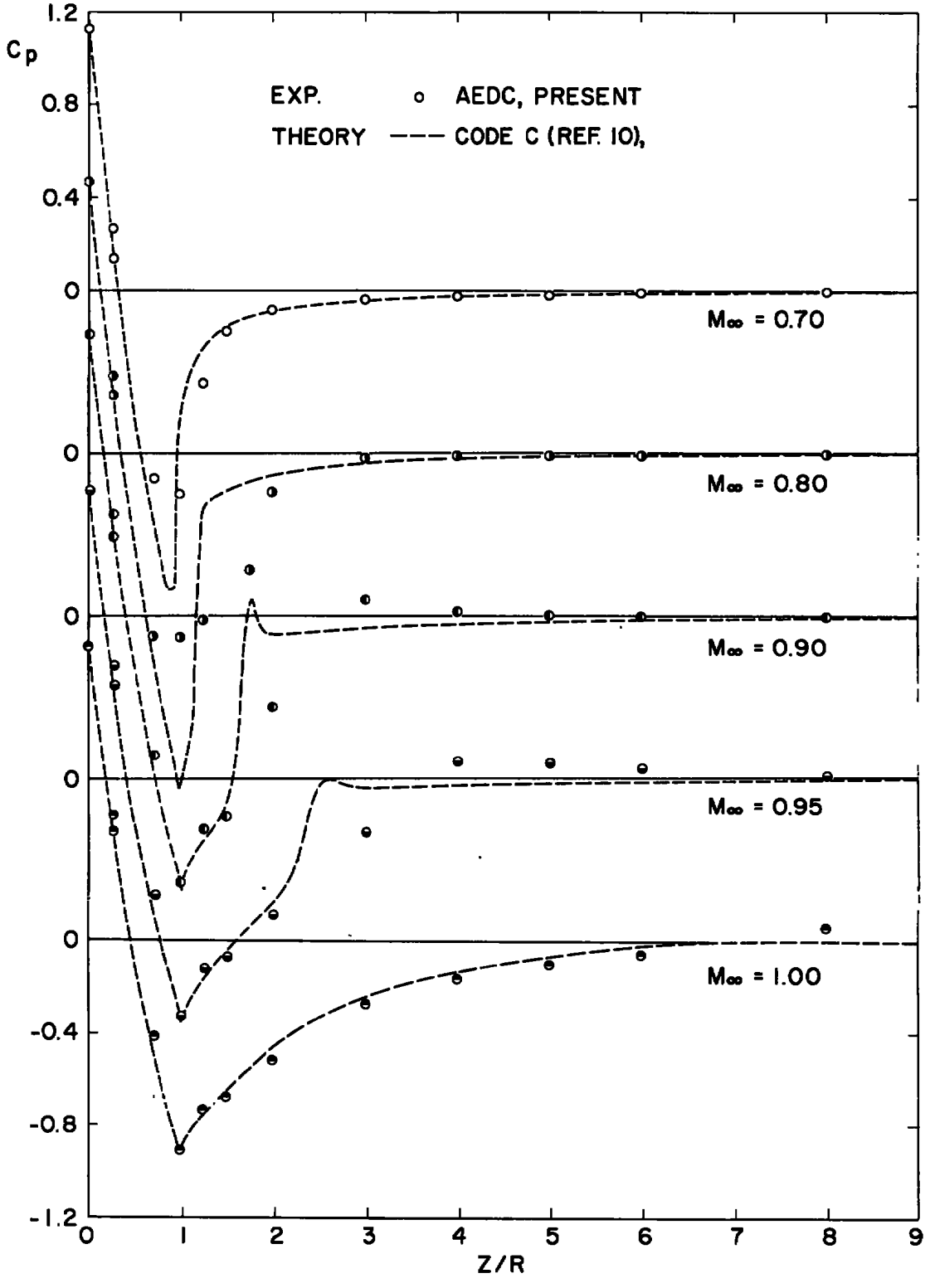

Figure 18. Comparison of calculated pressure with experiment.

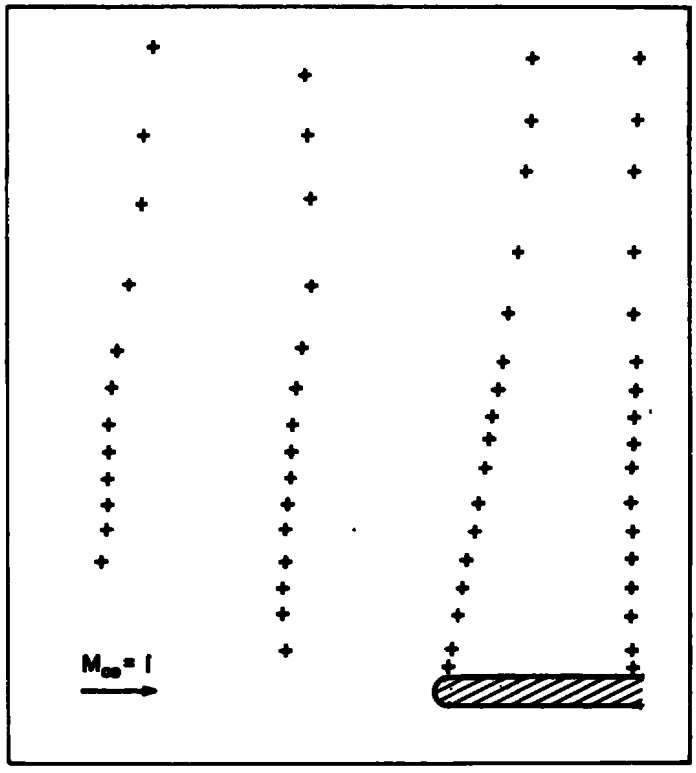

Figure 19. Calculated sonic line for M_∞ = 1 by method of Ref. 10.

5.0 CONCLUSIONS

From the above study of the flow field about a hemisphere-cylinder at zero incidence in the transonic and low supersonic Mach number range, the following conclusions can be drawn:

1. The inviscid theory can satisfactorily predict the flow field for $2 > M_\infty \geq 1.05$. The method used is a combination of time-dependent solution for the hemispherical nose portion and the method of characteristics for the cylindrical portion.

2. The relaxation method of Ref. 10 can satisfactorily predict the surface pressure for Mach numbers from 0.95 to 1.3, but the external flow field predicted is not as good as the surface pressure. For Mach numbers near 0.8, experimental results show an interaction of the shock and boundary layer; hence the inviscid theory fails to give satisfactory results.

REFERECES

1. Moretti, G. and Abbett, M. "A Time-Dependent Computational Method for Blunt Body Flows." AIAA Journal, Vol. 4, No. 12, December 1966, pp. 2136-2141.

2. Aungier, R. H. "A Computational Method for Exact, Direct and Unified Solutions for Axisymmetric Flow over Blunt Bodies of Arbitrary Shape (Program Blunt)." AFWL-TR-70-16, July 1970.

3. Moretti, G. "Inviscid Blunt Body Shock Layers." PIBAL 68-15, June 1968.

4. Abbett, M. J. "Finite Difference Solution of the Subsonic/Supersonic Inviscid Flow Field about a Supersonic, Axisymmetric Blunt Body at Aero Incidence-Analysis and User's Manual." SC-CR-71 5165, November 1971.

5. Gilïnskii, S. M. and Lebedev, M. G. "Investigation of a Flow at Low Supersonic Speeds–Past Plane and Axisymmetric Bodies with a Separated Shock Wave." Akademiia Nauk SSSR, Izvestiia Mekhanika, January - February 1965.

6. Van Dyke, M. D. and Gordon, H. D. "Supersonic Flow Past a Family of Blunt-Axisymmetric Bodies." NASA TR R-1, 1959.

7. Weilerstein, G. "The Addition of Secondary Shock Capability and Modifications to the GASL Three-Dimensional Characteristics Program, Part II. User's and Programmer's Manual." GASL-TR-653, August 1967.

8. Prozen, R. J. "Solution of Non-Isoenergetic Supersonic Flows by Method of Characteristics." HREC-7761-3-A, Lockheed Missiles and Space Co., Huntsville Research and Engineering Center, 1971.

9. Lipnitskii, Iu. M. and Lifshits. Iu. B. "Analysis of Transonic Flows Past Solids of Revolution." PMM. Vol. 34, No. 3, 1970, pp. 477-482.

10. South, J., Jr. and Jameson, A. Relaxation Solutions for Inviscid Axisymmetric Transonic Flow over Blunt or Pointed Bodies." Proceedings of the AIAA Computational Fluid Dynamics Conference, Palm Springs, California, July 19-20, 1973.

11. Stlip, A. Stromungsuntersuchungen an Kugeln mit transonischen und supersonischen Geschwindigkeiten in Luft and Frigen-Luftgemischen, Bericht Nr. 10/65, Ernst-Mach-Institut, Freiburg i. Br. Eckerstrasse 4, German, 1965.

12. Holder, D. W. and Chinneck, A. "The Flow Past Elliptic-nosed Cylinders and Bodies of Revolution in Supersonic Air Streams." The Aeronautical Quarterly, Vol. IV, February 1954, pp. 317-340.

13. Heberle, J. W., Wood, G. P., and Gooderum, P. B. "Data on Shape and Location of Detached Shock Waves on Cone and Spheres." NACA TN 2000, January 1950.

14. MacCormack, R. "The Effect of Viscosity in Hypervelocity Impact Cratering." AIAA Paper 69-354, presented at the AIAA Hypervelocity Impact Conference, Cincinnati, Ohio, April 30-May 2, 1969.

15. Eppright, B. R., Jr. "Theoretical Effects of Porosity and Angle of Attack on Jet Stretcher Performance." Ph.D. Dissertation, Texas A & M, University Microfilm, May 1971.

16. Jackson, F. M. and Sloan, E. H. "Calibration of the AEDC-PWT 1-Foot Transonic Tunnel. AEDC-TR-68-4 (AD827912), February 1968.

17. Murman, Earll M. "Analysis of Embedded Shock Waves Calculated by Relaxation Methods." Proceedings of the AIAA Computational Fluid Dynamics Conference, Palm Springs, California, July 19-20, 1973, pp. 27-40.

APPENDIX A
TABULATION OF FLOW QUANTITIES IN THE INITIAL PLAN AT TANGENT POINT ACROSS THE SHOCK LAYER

$M_\infty = 1.048$

R	U	V	RHO	P	M	T
1.00000E 00	1.71500E 00	0.0	5.44100E-01	4.35000E-01	1.62104E 00	7.99486E-01
1.17121E 00	1.56764E 00	1.07493E-01	6.89206E-01	5.97500E-01	1.42628E 00	8.66940E-01
1.34241E 00	1.40000E 00	1.91996E-01	8.13362E-01	7.60000E-01	1.23551E 00	9.34394E-01
1.51362E 00	1.34852E 00	1.84626E-01	8.74343E-01	8.35000E-01	1.17713E 00	9.55002E-01
1.68483E 00	1.29500E 00	1.77000E-01	9.32749E-01	9.10000E-01	1.11837E 00	9.75611E-01
1.85603E 00	1.26785E 00	1.66399E-01	9.55815E-01	9.42500E-01	1.08833E 00	9.86070E-01
2.02724E 00	1.24000E 00	1.56004E-01	9.78397E-01	9.75000E-01	1.05809E 00	9.96528E-01
2.19845E 00	1.23009E 00	1.45440E-01	9.92025E-01	9.92499E-01	1.04661E 00	1.00048E 00
2.36965E 00	1.22000E 00	1.35005E-01	1.00555E 00	1.01000E 00	1.03509E 00	1.00443E 00
2.54086E 00	1.21007E 00	1.26447E-01	1.01667E 00	1.02500E 00	1.02408E 00	1.00819E 00
2.71206E 00	1.20000E 00	1.17996E-01	1.02771E 00	1.04000E 00	1.01304E 00	1.01196E 00
2.88327E 00	1.19652E 00	1.11480E-01	1.03122E 00	1.04500E 00	1.00891E 00	1.01336E 00
3.05448E 00	1.19300E 00	1.04996E-01	1.03472E 00	1.05000E 00	1.00478E 00	1.01476E 00
3.22568E 00	1.19291E 00	9.99957E-02	1.03700E 00	1.05250E 00	1.00426E 00	1.01494E 00
3.39689E 00	1.19280E 00	9.49947E-02	1.03928E 00	1.05500E 00	1.00373E 00	1.01512E 00
3.56810E 00	1.19280E 00	9.24958E-02	1.03951E 00	1.05530E 00	1.00354E 00	1.01518E 00
3.73930E 00	1.19280E 00	8.99966E-02	1.03974E 00	1.05560E 00	1.00334E 00	1.01525E 00
3.91051E 00	1.19280E 00	8.60012E-02	1.03964E 00	1.05560E 00	1.00305E 00	1.01535E 00
4.08172E 00	1.19280E 00	8.20047E-02	1.03954E 00	1.05560E 00	1.00276E 00	1.01545E 00
4.25292E 00	1.19281E 00	7.80035E-02	1.03950E 00	1.05565E 00	1.00250E 00	1.01554E 00
4.42413E 00	1.19280E 00	7.40013E-02	1.03946E 00	1.05570E 00	1.00224E 00	1.01563E 00
4.59534E 00	1.19280E 00	7.15025E-02	1.03940E 00	1.05570E 00	1.00209E 00	1.01568E 00
4.76654E 00	1.19280E 00	6.90033E-02	1.03935E 00	1.05570E 00	1.00194E 00	1.01573E 00
4.93775E 00	1.19280E 00	6.60037E-02	1.03934E 00	1.05575E 00	1.00177E 00	1.01578E 00
5.10896E 00	1.19280E 00	6.30037E-02	1.03934E 00	1.05580E 00	1.00160E 00	1.01584E 00
5.28016E 00	1.19280E 00	6.09997E-02	1.03930E 00	1.05580E 00	1.00150E 00	1.01587E 00
5.45137E 00	1.19279E 00	5.89956E-02	1.03926E 00	1.05580E 00	1.00139E 00	1.01591E 00
5.62257E 00	1.19280E 00	5.69978E-02	1.03928E 00	1.05585E 00	1.00130E 00	1.01594E 00
5.79378E 00	1.19280E 00	5.49999E-02	1.03929E 00	1.05590E 00	1.00120E 00	1.01598E 00
5.96499E 00	1.19281E 00	5.37538E-02	1.03928E 00	1.05590E 00	1.00115E 00	1.01600E 00
6.13619E 00	1.19281E 00	5.25077E-02	1.03926E 00	1.05590E 00	1.00110E 00	1.01601E 00
6.30740E 00	1.19282E 00	5.12553E-02	1.03929E 00	1.05595E 00	1.00105E 00	1.01603E 00
6.47861E 00	1.19282E 00	5.00030E-02	1.03932E 00	1.05600E 00	1.00100E 00	1.01605E 00
6.64981E 00	1.19287E 00	4.90031E-02	1.03930E 00	1.05600E 00	1.00100E 00	1.01606E 00
6.82102E 00	1.19292E 00	4.80031E-02	1.03929E 00	1.05600E 00	1.00100E 00	1.01608E 00
6.99223E 00	1.19299E 00	4.65087E-02	1.03932E 00	1.05605E 00	1.00100E 00	1.01610E 00
7.16343E 00	1.19306E 00	4.50140E-02	1.03935E 00	1.05610E 00	1.00100E 00	1.01612E 00
7.33464E 00	1.19312E 00	4.35133E-02	1.03933E 00	1.05610E 00	1.00100E 00	1.01614E 00
7.50585E 00	1.19319E 00	4.20122E-02	1.03931E 00	1.05610E 00	1.00100E 00	1.01616E 00

*

*M values are slightly less than one, from the hemisphere solution, but are adjusted by slightly increasing U to fit the requirement of MOC calculation.

M_∞ = 1.048 (Continued)

R	U	V	RHO	P	M	T
7.67705E 00	1.19323E 00	4.10114E-02	1.03934E 00	1.05615E 00	1.00100E 00	1.01617E 00
7.84826E 00	1.19327E 00	4.00104E-02	1.03938E 00	1.05620E 00	1.00100E 00	1.01618E 00
8.01947E 00	1.19331E 00	3.90153E-02	1.03937E 00	1.05620E 00	1.00100E 00	1.01619E 00
8.19067E 00	1.19335E 00	3.80201E-02	1.03936E 00	1.05620E 00	1.00100E 00	1.01620E 00
8.36188E 00	1.19337E 00	3.75195E-02	1.03940E 00	1.05625E 00	1.00100E 00	1.01621E 00
8.53308E 00	1.19339E 00	3.70188E-02	1.03945E 00	1.05630E 00	1.00100E 00	1.01621E 00
8.70429E 00	1.19342E 00	3.60175E-02	1.03944E 00	1.05630E 00	1.00100E 00	1.01622E 00
8.87550E 00	1.19346E 00	3.50161E-02	1.03942E 00	1.05630E 00	1.00100E 00	1.01623E 00
9.04670E 00	1.19348E 00	3.45154E-02	1.03947E 00	1.05635E 00	1.00100E 00	1.01624E 00
9.21791E 00	1.19350E 00	3.40146E-02	1.03951E 00	1.05640E 00	1.00100E 00	1.01624E 00
9.38912E 00	1.19351E 00	3.35198E-02	1.03951E 00	1.05640E 00	1.00100E 00	1.01625E 00
9.56032E 00	1.19353E 00	3.30250E-02	1.03951E 00	1.05640E 00	1.00100E 00	1.01625E 00
9.73153E 00	1.19355E 00	3.25241E-02	1.03955E 00	1.05645E 00	1.00100E 00	1.01626E 00
9.90274E 00	1.19356E 00	3.20232E-02	1.03959E 00	1.05650E 00	1.00100E 00	1.01626E 00
1.00739E 01	1.19358E 00	3.15223E-02	1.03959E 00	1.05650E 00	1.00100E 00	1.01627E 00
1.02451E 01	1.19359E 00	3.10215E-02	1.03958E 00	1.05650E 00	1.00100E 00	1.01627E 00
1.04164E 01	1.19361E 00	3.05206E-02	1.03963E 00	1.05655E 00	1.00100E 00	1.01628E 00
1.05876E 01	1.19362E 00	3.00196E-02	1.03967E 00	1.05660E 00	1.00100E 00	1.01628E 00
1.07588E 01	1.19364E 00	2.95187E-02	1.03967E 00	1.05660E 00	1.00100E 00	1.01628E 00
1.09300E 01	1.19365E 00	2.90177E-02	1.03967E 00	1.05660E 00	1.00100E 00	1.01629E 00
1.11012E 01	1.19367E 00	2.85167E-02	1.03971E 00	1.05665E 00	1.00100E 00	1.01629E 00
1.12724E 01	1.19368E 00	2.80157E-02	1.03975E 00	1.05670E 00	1.00100E 00	1.01630E 00
1.14436E 01	1.19368E 00	2.75144E-02	1.03977E 00	1.05670E 00	1.00100E 00	1.01628E 00
1.16148E 01	1.19369E 00	2.70131E-02	1.03978E 00	1.05670E 00	1.00100E 00	1.01627E 00
1.17860E 01	1.19370E 00	2.67626E-02	1.03983E 00	1.05675E 00	1.00100E 00	1.01627E 00
1.19572E 01	1.19370E 00	2.65121E-02	1.03988E 00	1.05680E 00	1.00100E 00	1.01627E 00
1.21284E 01	1.19371E 00	2.62676E-02	1.03988E 00	1.05680E 00	1.00100E 00	1.01628E 00
1.22996E 01	1.19371E 00	2.60230E-02	1.03987E 00	1.05680E 00	1.00100E 00	1.01628E 00
1.24708E 01	1.19373E 00	2.55219E-02	1.03992E 00	1.05685E 00	1.00100E 00	1.01628E 00
1.26420E 01	1.19374E 00	2.50208E-02	1.03996E 00	1.05690E 00	1.00100E 00	1.01628E 00
1.28132E 01	1.19375E 00	2.45197E-02	1.03996E 00	1.05690E 00	1.00100E 00	1.01629E 00
1.29845E 01	1.19377E 00	2.40186E-02	1.03996E 00	1.05690E 00	1.00100E 00	1.01629E 00
1.31557E 01	1.19377E 00	2.37680E-02	1.04000E 00	1.05695E 00	1.00100E 00	1.01629E 00
1.33269E 01	1.19378E 00	2.35174E-02	1.04005E 00	1.05700E 00	1.00100E 00	1.01629E 00
1.34981E 01	1.19378E 00	2.32668E-02	1.04005E 00	1.05700E 00	1.00100E 00	1.01629E 00
1.36693E 01	1.19379E 00	2.30162E-02	1.04005E 00	1.05700E 00	1.00100E 00	1.01630E 00
1.38405E 01	1.19380E 00	2.25151E-02	1.04009E 00	1.05705E 00	1.00100E 00	1.01630E 00
1.40117E 01	1.19382E 00	2.20139E-02	1.04014E 00	1.05710E 00	1.00100E 00	1.01630E 00
1.41829E 01	1.19382E 00	2.20139E-02	1.04014E 00	1.05710E 00	1.00100E 00	1.01630E 00

*

All M values are slightly less than one, from the hemisphere solution, but are adjusted by slightly increasing U to fit the requirement of MOC calculation.

M_∞ = 1.048 (Concluded)

R	U	V	RHO	P	M	T	
1.43541E 01	1.19382E 00	2.20139E-02	1.04014E 00	1.05710E 00	1.00100E 00	1.01630E 00	
1.45253E 01	1.19382E 00	2.20139E-02	1.04019E 00	1.05715E 00	1.00100E 00	1.01630E 00	
1.46965E 01	1.19382E 00	2.20139E-02	1.04024E 00	1.05720E 00	1.00100E 00	1.01630E 00	
1.48677E 01	1.19382E 00	2.20139E-02	1.04024E 00	1.05720E 00	1.00100E 00	1.01630E 00	
1.50389E 01	1.19382E 00	2.20139E-02	1.04024E 00	1.05720E 00	1.00100E 00	1.01630E 00	
1.52101E 01	1.19381E 00	2.15125E-02	1.04030E 00	1.05725E 00	1.00100E 00	1.01629E 00	
1.53813E 01	1.19381E 00	2.10111E-02	1.04037E 00	1.05730E 00	1.00100E 00	1.01628E 00	
1.55526E 01	1.19381E 00	2.10111E-02	1.04035E 00	1.05728E 00	1.00100E 00	1.01628E 00	*
1.57238E 01	1.19381E 00	2.10111E-02	1.04033E 00	1.05727E 00	1.00100E 00	1.01628E 00	
1.58950E 01	1.19381E 00	2.10111E-02	1.04020E 00	1.05713E 00	1.00100E 00	1.01628E 00	
1.60662E 01	1.19381E 00	2.10111E-02	1.04007E 00	1.05700E 00	1.00100E 00	1.01628E 00	
1.62374E 01	1.19378E 00	2.10105E-02	1.04013E 00	1.05700E 00	1.00100E 00	1.01622E 00	
1.64086E 01	1.19375E 00	2.10099E-02	1.04019E 00	1.05701E 00	1.00099E 00	1.01617E 00	
1.65798E 01	1.19375E 00	2.05086E-02	1.04020E 00	1.05700E 00	1.00100E 00	1.01616E 00	
1.67510E 01	1.19375E 00	2.00073E-02	1.04020E 00	1.05700E 00	1.00100E 00	1.01615E 00	
1.69222E 01	1.19382E 00	2.00025E-02	1.04004E 00	1.05675E 00	1.00110E 00	1.01606E 00	
1.70934E 01	1.19390E 00	1.99978E-02	1.03988E 00	1.05650E 00	1.00120E 00	1.01598E 00	
1.72646E 01	1.19410E 00	1.94997E-02	1.03971E 00	1.05625E 00	1.00140E 00	1.01591E 00	
1.74358E 01	1.19431E 00	1.90014E-02	1.03954E 00	1.05601E 00	1.00160E 00	1.01584E 00	
1.76070E 01	1.19450E 00	1.89986E-02	1.03936E 00	1.05575E 00	1.00180E 00	1.01577E 00	
1.77782E 01	1.19470E 00	1.89957E-02	1.03917E 00	1.05550E 00	1.00199E 00	1.01571E 00	
1.79494E 01	1.19495E 00	1.87488E-02	1.03902E 00	1.05525E 00	1.00225E 00	1.01562E 00	
1.81206E 01	1.19521E 00	1.85018E-02	1.03887E 00	1.05501E 00	1.00250E 00	1.01554E 00	
1.82918E 01	1.19540E 00	1.84989E-02	1.03868E 00	1.05475E 00	1.00270E 00	1.01547E 00	
1.84630E 01	1.19560E 00	1.84959E-02	1.03850E 00	1.05450E 00	1.00289E 00	1.01540E 00	
1.86342E 01	1.19585E 00	1.82487E-02	1.03834E 00	1.05425E 00	1.00314E 00	1.01532E 00	
1.88054E 01	1.19610E 00	1.80013E-02	1.03818E 00	1.05400E 00	1.00339E 00	1.01523E 00	
1.89766E 01	1.19635E 00	1.79992E-02	1.03803E 00	1.05375E 00	1.00365E 00	1.01515E 00	
1.91478E 01	1.19661E 00	1.79970E-02	1.03788E 00	1.05351E 00	1.00390E 00	1.01506E 00	
1.93190E 01	1.19680E 00	1.77486E-02	1.03769E 00	1.05325E 00	1.00409E 00	1.01500E 00	
1.94902E 01	1.19700E 00	1.75001E-02	1.03751E 00	1.05300E 00	1.00428E 00	1.01493E 00	
1.96614E 01	1.19720E 00	1.75031E-02	1.03734E 00	1.05275E 00	1.00449E 00	1.01486E 00	
1.98326E 01	1.19741E 00	1.75061E-02	1.03717E 00	1.05251E 00	1.00470E 00	1.01479E 00	
2.00038E 01	1.19765E 00	1.72522E-02	1.03700E 00	1.05225E 00	1.00494E 00	1.01471E 00	
2.01750E 01	1.19790E 00	1.69982E-02	1.03683E 00	1.05200E 00	1.00519E 00	1.01462E 00	
2.03463E 01	1.19795E 00	1.67473E-02	1.03685E 00	1.05200E 00	1.00524E 00	1.01461E 00	
2.05175E 01	1.19800E 00	1.64965E-02	1.03687E 00	1.05200E 00	1.00528E 00	1.01459E 00	
2.06887E 01	1.19807E 00	1.62458E-02	1.03691E 00	1.05201E 00	1.00535E 00	1.01457E 00	
2.08599E 01	1.19814E 00	1.59951E-02	1.03694E 00	1.05203E 00	1.00541E 00	1.01455E 00	

*M values are slightly less than one, from the hemisphere solution, but are adjusted by slightly increasing U to fit the requirement of MOC calculation.

$M_\infty = 1.1$

R	U	V	RHO	P	M	T	
1.00000E 00	1.78576E 00	0.0	5.47090E-01	4.30000E-01	1.70237E 00	7.85577E-01	
1.10595E 00	1.68928E 00	6.78449E-02	6.33118E-01	5.27505E-01	1.56537E 00	8.33185E-01	
1.21189E 00	1.59763E 00	1.28330E-01	7.14706E-01	6.25010E-01	1.44854E 00	8.74499E-01	
1.31784E 00	1.50905E 00	1.81820E-01	7.92733E-01	7.22515E-01	1.34558E 00	9.11423E-01	
1.42379E 00	1.42245E 00	2.28516E-01	8.67808E-01	8.20020E-01	1.25258E 00	9.44932E-01	
1.52974E 00	1.39563E 00	2.12317E-01	8.95377E-01	8.56645E-01	1.21977E 00	9.56743E-01	
1.63568E 00	1.36894E 00	1.96593E-01	9.22613E-01	8.93270E-01	1.18788E 00	9.68195E-01	
1.74163E 00	1.34234E 00	1.81337E-01	9.49537E-01	9.29895E-01	1.15682E 00	9.79314E-01	
1.84758E 00	1.31580E 00	1.66540E-01	9.76161E-01	9.66520E-01	1.12650E 00	9.90124E-01	
1.95353E 00	1.29805E 00	1.64407E-01	9.93030E-01	9.89899E-01	1.10756E 00	9.96847E-01	
2.05947E 00	1.28036E 00	1.62279E-01	1.00979E 00	1.01328E 00	1.08888E 00	1.00346E 00	
2.16542E 00	1.26272E 00	1.60154E-01	1.02643E 00	1.03666E 00	1.07043E 00	1.00996E 00	
2.27137E 00	1.24513E 00	1.58032E-01	1.04298E 00	1.06004E 00	1.05220E 00	1.01636E 00	
2.37732E 00	1.24348E 00	1.49301E-01	1.04568E 00	1.06379E 00	1.04943E 00	1.01732E 00	
2.48326E 00	1.24177E 00	1.40587E-01	1.04838E 00	1.06755E 00	1.04666E 00	1.01829E 00	
2.58921E 00	1.24001E 00	1.31890E-01	1.05107E 00	1.07131E 00	1.04391E 00	1.01926E 00	
2.69516E 00	1.23818E 00	1.23212E-01	1.05376E 00	1.07507E 00	1.04115E 00	1.02022E 00	
2.80111E 00	1.23223E 00	1.21061E-01	1.05960E 00	1.08332E 00	1.03492E 00	1.02239E 00	
2.90705E 00	1.22628E 00	1.18924E-01	1.06542E 00	1.09157E 00	1.02870E 00	1.02455E 00	
3.01300E 00	1.22033E 00	1.16804E-01	1.07122E 00	1.09983E 00	1.02252E 00	1.02670E 00	
3.11895E 00	1.21438E 00	1.14698E-01	1.07702E 00	1.10808E 00	1.01635E 00	1.02884E 00	
3.22490E 00	1.21498E 00	1.09901E-01	1.07707E 00	1.10808E 00	1.01651E 00	1.02879E 00	
3.33084E 00	1.21557E 00	1.05098E-01	1.07713E 00	1.10808E 00	1.01667E 00	1.02873E 00	
3.43679E 00	1.21613E 00	1.00288E-01	1.07719E 00	1.10808E 00	1.01683E 00	1.02868E 00	
3.54274E 00	1.21667E 00	9.54723E-02	1.07725E 00	1.10808E 00	1.01698E 00	1.02862E 00	
3.64869E 00	1.21648E 00	9.40889E-02	1.07771E 00	1.10867E 00	1.01669E 00	1.02872E 00	
3.75463E 00	1.21629E 00	9.27056E-02	1.07818E 00	1.10926E 00	1.01639E 00	1.02883E 00	
3.86058E 00	1.21609E 00	9.13225E-02	1.07865E 00	1.10986E 00	1.01608E 00	1.02893E 00	
3.96653E 00	1.21589E 00	8.99396E-02	1.07911E 00	1.11045E 00	1.01578E 00	1.02904E 00	
4.07248E 00	1.21443E 00	8.69128E-02	1.08084E 00	1.11286E 00	1.01409E 00	1.02962E 00	
4.17842E 00	1.21295E 00	8.38937E-02	1.08256E 00	1.11527E 00	1.01240E 00	1.03021E 00	
4.28437E 00	1.21147E 00	8.08798E-02	1.08429E 00	1.11768E 00	1.01071E 00	1.03079E 00	
4.39032E 00	1.20997E 00	7.78738E-02	1.08601E 00	1.12009E 00	1.00902E 00	1.03138E 00	
4.49627E 00	1.21019E 00	7.67803E-02	1.08606E 00	1.12009E 00	1.00916E 00	1.03133E 00	*
4.60221E 00	1.21040E 00	7.56860E-02	1.08611E 00	1.12009E 00	1.00930E 00	1.03128E 00	*
4.70816E 00	1.21060E 00	7.45914E-02	1.08617E 00	1.12009E 00	1.00945E 00	1.03123E 00	*
4.81411E 00	1.21081E 00	7.34961E-02	1.08622E 00	1.12009E 00	1.00958E 00	1.03118E 00	*
4.92006E 00	1.21106E 00	7.16848E-02	1.08627E 00	1.12009E 00	1.00972E 00	1.03114E 00	*
5.02600E 00	1.21130E 00	6.98736E-02	1.08632E 00	1.12009E 00	1.00986E 00	1.03109E 00	*

*Mach numbers are slightly less than one, from the hemisphere solution, but are adjusted by slightly increasing U to fit the requirement of MOC calculation.

M_∞ = 1.1 (Continued)

R	U	V	RHO	P	M	T
5.13195E 00	1.21153E 00	6.80603E-02	1.08636E 00	1.12009E 00	1.00999E 00	1.03104E 00
5.23790E 00	1.21177E 00	6.62473E-02	1.08641E 00	1.12009E 00	1.01012E 00	1.03100E 00
5.34385E 00	1.21195E 00	6.53628E-02	1.08646E 00	1.12009E 00	1.01026E 00	1.03095E 00
5.44979E 00	1.21212E 00	6.44788E-02	1.08651E 00	1.12009E 00	1.01038E 00	1.03091E 00
5.55574E 00	1.21230E 00	6.35935E-02	1.08655E 00	1.12009E 00	1.01051E 00	1.03086E 00
5.66169E 00	1.21247E 00	6.27090E-02	1.08660E 00	1.12009E 00	1.01064E 00	1.03082E 00
5.76764E 00	1.21316E 00	6.15313E-02	1.08619E 00	1.11943E 00	1.01126E 00	1.03060E 00
5.87358E 00	1.21384E 00	6.03521E-02	1.08578E 00	1.11877E 00	1.01189E 00	1.03039E 00
5.97953E 00	1.21452E 00	5.91714E-02	1.08536E 00	1.11811E 00	1.01251E 00	1.03017E 00
6.08548E 00	1.21520E 00	5.79892E-02	1.08495E 00	1.11745E 00	1.01313E 00	1.02995E 00
6.19143E 00	1.21485E 00	5.72377E-02	1.08545E 00	1.11811E 00	1.01275E 00	1.03009E 00
6.29737E 00	1.21450E 00	5.64865E-02	1.08595E 00	1.11877E 00	1.01237E 00	1.03022E 00
6.40332E 00	1.21415E 00	5.57356E-02	1.08645E 00	1.11943E 00	1.01198E 00	1.03035E 00
6.50927E 00	1.21380E 00	5.49850E-02	1.08695E 00	1.12009E 00	1.01159E 00	1.03049E 00
6.61522E 00	1.21395E 00	5.41724E-02	1.08699E 00	1.12009E 00	1.01171E 00	1.03045E 00
6.72116E 00	1.21410E 00	5.33595E-02	1.08703E 00	1.12009E 00	1.01182E 00	1.03041E 00
6.82711E 00	1.21424E 00	5.25462E-02	1.08707E 00	1.12009E 00	1.01193E 00	1.03037E 00
6.93306E 00	1.21438E 00	5.17326E-02	1.08711E 00	1.12009E 00	1.01203E 00	1.03034E 00
7.03901E 00	1.21451E 00	5.11249E-02	1.08715E 00	1.12009E 00	1.01214E 00	1.03030E 00
7.14495E 00	1.21464E 00	5.05170E-02	1.08719E 00	1.12009E 00	1.01225E 00	1.03026E 00
7.25090E 00	1.21477E 00	4.99088E-02	1.08722E 00	1.12009E 00	1.01235E 00	1.03023E 00
7.35685E 00	1.21490E 00	4.93005E-02	1.08726E 00	1.12009E 00	1.01245E 00	1.03019E 00
7.46280E 00	1.21502E 00	4.87186E-02	1.08730E 00	1.12009E 00	1.01255E 00	1.03016E 00
7.56874E 00	1.21514E 00	4.81378E-02	1.08733E 00	1.12009E 00	1.01265E 00	1.03012E 00
7.67469E 00	1.21526E 00	4.75555E-02	1.08737E 00	1.12009E 00	1.01274E 00	1.03009E 00
7.78064E 00	1.21538E 00	4.69744E-02	1.08740E 00	1.12009E 00	1.01284E 00	1.03006E 00
7.88659E 00	1.21599E 00	4.64934E-02	1.08698E 00	1.11943E 00	1.01344E 00	1.02985E 00
7.99253E 00	1.21660E 00	4.60119E-02	1.08656E 00	1.11877E 00	1.01403E 00	1.02965E 00
8.09848E 00	1.21721E 00	4.55297E-02	1.08613E 00	1.11811E 00	1.01462E 00	1.02944E 00
8.20443E 00	1.21781E 00	4.50470E-02	1.08571E 00	1.11745E 00	1.01521E 00	1.02924E 00
8.31038E 00	1.21799E 00	4.46173E-02	1.08567E 00	1.11736E 00	1.01537E 00	1.02918E 00
8.41632E 00	1.21815E 00	4.41886E-02	1.08565E 00	1.11727E 00	1.01552E 00	1.02913E 00
8.52227E 00	1.21832E 00	4.37586E-02	1.08561E 00	1.11718E 00	1.01568E 00	1.02908E 00
8.62822E 00	1.21849E 00	4.33295E-02	1.08558E 00	1.11709E 00	1.01583E 00	1.02902E 00
8.73417E 00	1.21859E 00	4.29150E-02	1.08561E 00	1.11709E 00	1.01591E 00	1.02900E 00
8.84011E 00	1.21868E 00	4.25015E-02	1.08564E 00	1.11709E 00	1.01599E 00	1.02897E 00
8.94606E 00	1.21877E 00	4.20866E-02	1.08567E 00	1.11709E 00	1.01607E 00	1.02894E 00
9.05201E 00	1.21886E 00	4.16729E-02	1.08569E 00	1.11709E 00	1.01614E 00	1.02891E 00
9.15796E 00	1.21933E 00	4.13498E-02	1.08538E 00	1.11659E 00	1.01660E 00	1.02876E 00

*Mach numbers are slightly less than one, from the hemisphere solution, but are adjusted by slightly increasing U to fit the requirement of MOC calculation.

M_∞ = 1.1 (Concluded)

R	U	V	RHO	P	M	T
9.26390E 00	1.21979E 00	4.10276E-02	1.08506E 00	1.11609E 00	1.01705E 00	1.02860E 00
9.36985E 00	1.22025E 00	4.07039E-02	1.08473E 00	1.11559E 00	1.01750E 00	1.02844E 00
9.47580E 00	1.22071E 00	4.03810E-02	1.08441E 00	1.11509E 00	1.01795E 00	1.02829E 00
9.58175E 00	1.22097E 00	4.00297E-02	1.08427E 00	1.11484E 00	1.01821E 00	1.02820E 00
9.68769E 00	1.22124E 00	3.96782E-02	1.08412E 00	1.11459E 00	1.01847E 00	1.02811E 00
9.79364E 00	1.22151E 00	3.93265E-02	1.08397E 00	1.11434E 00	1.01872E 00	1.02802E 00
9.89959E 00	1.22177E 00	3.89745E-02	1.08382E 00	1.11409E 00	1.01898E 00	1.02793E 00
1.00055E 01	1.22272E 00	3.87419E-02	1.08303E 00	1.11293E 00	1.01992E 00	1.02760E 00
1.01115E 01	1.22366E 00	3.85086E-02	1.08225E 00	1.11177E 00	1.02087E 00	1.02728E 00
1.02174E 01	1.22460E 00	3.82750E-02	1.08147E 00	1.11062E 00	1.02180E 00	1.02695E 00
1.03234E 01	1.22554E 00	3.80408E-02	1.08069E 00	1.10946E 00	1.02274E 00	1.02662E 00
1.04293E 01	1.22437E 00	3.76923E-02	1.08184E 00	1.11109E 00	1.02155E 00	1.02704E 00
1.05353E 01	1.22320E 00	3.73444E-02	1.08300E 00	1.11273E 00	1.02037E 00	1.02745E 00
1.06412E 01	1.22203E 00	3.69970E-02	1.08416E 00	1.11436E 00	1.01918E 00	1.02786E 00
1.07472E 01	1.22086E 00	3.66502E-02	1.08531E 00	1.11600E 00	1.01799E 00	1.02827E 00
1.08531E 01	1.21858E 00	3.63684E-02	1.08748E 00	1.11910E 00	1.01568E 00	1.02907E 00
1.09591E 01	1.21629E 00	3.60873E-02	1.08965E 00	1.12220E 00	1.01338E 00	1.02987E 00
1.10650E 01	1.21401E 00	3.58071E-02	1.09182E 00	1.12530E 00	1.01108E 00	1.03067E 00
1.11710E 01	1.21172E 00	3.55275E-02	1.09399E 00	1.12841E 00	1.00878E 00	1.03146E 00
1.12769E 01	1.21442E 00	3.53300E-02	1.09157E 00	1.12489E 00	1.01149E 00	1.03053E 00
1.13829E 01	1.21713E 00	3.51323E-02	1.08914E 00	1.12137E 00	1.01419E 00	1.02959E 00
1.14888E 01	1.21983E 00	3.49322E-02	1.08672E 00	1.11785E 00	1.01690E 00	1.02865E 00
1.15947E 01	1.22253E 00	3.47320E-02	1.08429E 00	1.11434E 00	1.01961E 00	1.02771E 00
1.17007E 01	1.22767E 00	3.47088E-02	1.07960E 00	1.10757E 00	1.02479E 00	1.02591E 00
1.18066E 01	1.23282E 00	3.46853E-02	1.07489E 00	1.10081E 00	1.02999E 00	1.02411E 00
1.19126E 01	1.23796E 00	3.46592E-02	1.07019E 00	1.09404E 00	1.03520E 00	1.02229E 00
1.20185E 01	1.24311E 00	3.46329E-02	1.06547E 00	1.08728E 00	1.04043E 00	1.02047E 00
1.21245E 01	1.23616E 00	3.41736E-02	1.07195E 00	1.09654E 00	1.03336E 00	1.02293E 00
1.22304E 01	1.22921E 00	3.37172E-02	1.07842E 00	1.10579E 00	1.02632E 00	1.02538E 00
1.23364E 01	1.22227E 00	3.32640E-02	1.08487E 00	1.11505E 00	1.01931E 00	1.02782E 00
1.24423E 01	1.21532E 00	3.28136E-02	1.09131E 00	1.12431E 00	1.01231E 00	1.03024E 00
1.25483E 01	1.21781E 00	3.27553E-02	1.08906E 00	1.12105E 00	1.01481E 00	1.02938E 00
1.26542E 01	1.22029E 00	3.26978E-02	1.08680E 00	1.11779E 00	1.01731E 00	1.02851E 00
1.27602E 01	1.22278E 00	3.26383E-02	1.08455E 00	1.11453E 00	1.01980E 00	1.02765E 00
1.28661E 01	1.22526E 00	3.25796E-02	1.08229E 00	1.11127E 00	1.02230E 00	1.02678E 00
1.29721E 01	1.22812E 00	3.23794E-02	1.07968E 00	1.10751E 00	1.02518E 00	1.02578E 00
1.30780E 01	1.23098E 00	3.21778E-02	1.07707E 00	1.10375E 00	1.02806E 00	1.02478E 00
1.31840E 01	1.23384E 00	3.19748E-02	1.07445E 00	1.10000E 00	1.03095E 00	1.02377E 00
1.32900E 01	1.23669E 00	3.17706E-02	1.07183E 00	1.09624E 00	1.03384E 00	1.02277E 00

$M_\infty = 1.2$

R	U	V	RHO	P	M	T
1.00000E 00	1.82907E 00	0.0	5.76547E-01	4.63900E-01	1.72334E 00	8.04618E-01
1.05941E 00	1.75940E 00	7.35782E-02	6.54451E-01	5.49295E-01	1.62449E 00	8.39322E-01
1.11883E 00	1.68419E 00	1.40867E-01	7.26166E-01	6.34690E-01	1.52784E 00	8.74028E-01
1.17824E 00	1.63203E 00	1.74098E-01	7.91278E-01	7.09845E-01	1.46455E 00	8.97087E-01
1.23765E 00	1.57779E 00	2.04659E-01	8.53126E-01	7.85000E-01	1.40178E 00	9.20145E-01
1.29706E 00	1.54038E 00	2.14520E-01	8.76798E-01	8.20780E-01	1.35854E 00	9.36110E-01
1.35648E 00	1.50210E 00	2.23537E-01	8.99676E-01	8.56560E-01	1.31540E 00	9.52076E-01
1.41589E 00	1.47567E 00	2.21624E-01	9.27245E-01	8.93280E-01	1.28490E 00	9.63370E-01
1.47530E 00	1.44876E 00	2.19570E-01	9.54178E-01	9.30000E-01	1.25440E 00	9.74661E-01
1.53472E 00	1.42880E 00	2.17328E-01	9.74999E-01	9.58375E-01	1.23199E 00	9.82949E-01
1.59413E 00	1.40856E 00	2.15023E-01	9.95472E-01	9.86750E-01	1.20956E 00	9.91238E-01
1.65354E 00	1.39385E 00	2.11181E-01	1.01108E 00	1.00837E 00	1.19306E 00	9.97323E-01
1.71296E 00	1.37897E 00	2.07348E-01	1.02650E 00	1.03000E 00	1.17654E 00	1.00341E 00
1.77237E 00	1.36737E 00	2.04071E-01	1.03879E 00	1.04722E 00	1.16373E 00	1.00811E 00
1.83178E 00	1.35567E 00	2.00805E-01	1.05096E 00	1.06444E 00	1.15090E 00	1.01282E 00
1.89119E 00	1.34656E 00	1.97437E-01	1.06071E 00	1.07822E 00	1.14084E 00	1.01651E 00
1.95061E 00	1.33737E 00	1.94086E-01	1.07038E 00	1.09200E 00	1.13077E 00	1.02019E 00
2.01002E 00	1.32944E 00	1.90658E-01	1.07892E 00	1.10415E 00	1.12203E 00	1.02338E 00
2.06943E 00	1.32144E 00	1.87249E-01	1.08741E 00	1.11631E 00	1.11328E 00	1.02658E 00
2.12885E 00	1.31478E 00	1.83808E-01	1.09463E 00	1.12665E 00	1.10594E 00	1.02925E 00
2.18826E 00	1.30807E 00	1.80387E-01	1.10182E 00	1.13700E 00	1.09858E 00	1.03192E 00
2.24767E 00	1.30232E 00	1.76937E-01	1.10810E 00	1.14603E 00	1.09224E 00	1.03422E 00
2.30709E 00	1.29654E 00	1.73506E-01	1.11436E 00	1.15506E 00	1.08589E 00	1.03653E 00
2.36650E 00	1.29186E 00	1.70209E-01	1.11953E 00	1.16253E 00	1.08070E 00	1.03841E 00
2.42591E 00	1.28715E 00	1.66928E-01	1.12469E 00	1.17000E 00	1.07550E 00	1.04029E 00
2.48532E 00	1.28385E 00	1.63952E-01	1.12843E 00	1.17540E 00	1.07178E 00	1.04163E 00
2.54474E 00	1.28054E 00	1.60988E-01	1.13216E 00	1.18081E 00	1.06806E 00	1.04297E 00
2.60415E 00	1.27776E 00	1.58292E-01	1.13533E 00	1.18540E 00	1.06493E 00	1.04411E 00
2.66356E 00	1.27497E 00	1.55606E-01	1.13850E 00	1.19000E 00	1.06179E 00	1.04524E 00
2.72298E 00	1.27164E 00	1.53241E-01	1.14215E 00	1.19531E 00	1.05816E 00	1.04654E 00
2.78239E 00	1.26830E 00	1.50886E-01	1.14580E 00	1.20063E 00	1.05453E 00	1.04785E 00
2.84180E 00	1.26537E 00	1.48790E-01	1.14902E 00	1.20531E 00	1.05136E 00	1.04899E 00
2.90121E 00	1.26244E 00	1.46703E-01	1.15224E 00	1.21000E 00	1.04818E 00	1.05013E 00
2.96063E 00	1.26066E 00	1.44838E-01	1.15428E 00	1.21297E 00	1.04620E 00	1.05084E 00
3.02004E 00	1.25889E 00	1.42978E-01	1.15633E 00	1.21594E 00	1.04422E 00	1.05155E 00
3.07945E 00	1.25774E 00	1.41298E-01	1.15773E 00	1.21797E 00	1.04288E 00	1.05203E 00
3.13887E 00	1.25659E 00	1.39621E-01	1.15913E 00	1.22000E 00	1.04155E 00	1.05251E 00
3.19828E 00	1.25585E 00	1.38094E-01	1.16011E 00	1.22140E 00	1.04065E 00	1.05283E 00
3.25769E 00	1.25511E 00	1.36570E-01	1.16109E 00	1.22281E 00	1.03974E 00	1.05315E 00

M_∞ = 1.2 (Continued)

R	U	V	RHO	P	M	T
3.31711E 00	1.25457E 00	1.35125E-01	1.16186E 00	1.22390E 00	1.03905E 00	1.05340E 00
3.37652E 00	1.25403E 00	1.33683E-01	1.16262E 00	1.22500E 00	1.03836E 00	1.05365E 00
3.43593E 00	1.25327E 00	1.32270E-01	1.16360E 00	1.22640E 00	1.03746E 00	1.05397E 00
3.49534E 00	1.25250E 00	1.30859E-01	1.16458E 00	1.22781E 00	1.03655E 00	1.05430E 00
3.55476E 00	1.25196E 00	1.29399E-01	1.16534E 00	1.22890E 00	1.03586E 00	1.05455E 00
3.61417E 00	1.25141E 00	1.27939E-01	1.16611E 00	1.23000E 00	1.03517E 00	1.05479E 00
3.67358E 00	1.25163E 00	1.26277E-01	1.16613E 00	1.23000E 00	1.03522E 00	1.05477E 00
3.73300E 00	1.25186E 00	1.24616E-01	1.16615E 00	1.23000E 00	1.03528E 00	1.05475E 00
3.79241E 00	1.25208E 00	1.22919E-01	1.16617E 00	1.23000E 00	1.03533E 00	1.05473E 00
3.85182E 00	1.25230E 00	1.21223E-01	1.16619E 00	1.23000E 00	1.03539E 00	1.05471E 00
3.91123E 00	1.25250E 00	1.19714E-01	1.16621E 00	1.23000E 00	1.03544E 00	1.05470E 00
3.97065E 00	1.25270E 00	1.18204E-01	1.16623E 00	1.23000E 00	1.03549E 00	1.05468E 00
4.03006E 00	1.25288E 00	1.16744E-01	1.16625E 00	1.23000E 00	1.03554E 00	1.05466E 00
4.08947E 00	1.25307E 00	1.15283E-01	1.16627E 00	1.23000E 00	1.03559E 00	1.05464E 00
4.14889E 00	1.25326E 00	1.13765E-01	1.16629E 00	1.23000E 00	1.03565E 00	1.05462E 00
4.20830E 00	1.25345E 00	1.12246E-01	1.16631E 00	1.23000E 00	1.03570E 00	1.05460E 00
4.26771E 00	1.25363E 00	1.10789E-01	1.16633E 00	1.23000E 00	1.03574E 00	1.05459E 00
4.32713E 00	1.25380E 00	1.09331E-01	1.16635E 00	1.23000E 00	1.03579E 00	1.05457E 00
4.38654E 00	1.25396E 00	1.08029E-01	1.16637E 00	1.23000E 00	1.03584E 00	1.05455E 00
4.44595E 00	1.25412E 00	1.06726E-01	1.16639E 00	1.23000E 00	1.03589E 00	1.05454E 00
4.50536E 00	1.25427E 00	1.05546E-01	1.16641E 00	1.23000E 00	1.03593E 00	1.05452E 00
4.56478E 00	1.25441E 00	1.04367E-01	1.16643E 00	1.23000E 00	1.03598E 00	1.05450E 00
4.62419E 00	1.25454E 00	1.03311E-01	1.16644E 00	1.23000E 00	1.03602E 00	1.05449E 00
4.68360E 00	1.25467E 00	1.02256E-01	1.16646E 00	1.23000E 00	1.03606E 00	1.05447E 00
4.74302E 00	1.25479E 00	1.01324E-01	1.16648E 00	1.23000E 00	1.03611E 00	1.05446E 00
4.80243E 00	1.25491E 00	1.00393E-01	1.16649E 00	1.23000E 00	1.03615E 00	1.05444E 00
4.86184E 00	1.25486E 00	9.95733E-02	1.16666E 00	1.23022E 00	1.03604E 00	1.05448E 00
4.92126E 00	1.25482E 00	9.87540E-02	1.16682E 00	1.23044E 00	1.03593E 00	1.05452E 00
4.98067E 00	1.25472E 00	9.80561E-02	1.16703E 00	1.23072E 00	1.03578E 00	1.05457E 00
5.04008E 00	1.25462E 00	9.73583E-02	1.16723E 00	1.23100E 00	1.03562E 00	1.05463E 00
5.09949E 00	1.25450E 00	9.68513E-02	1.16744E 00	1.23128E 00	1.03547E 00	1.05468E 00
5.15891E 00	1.25439E 00	9.63455E-02	1.16764E 00	1.23156E 00	1.03531E 00	1.05474E 00
5.21832E 00	1.25431E 00	9.58330E-02	1.16780E 00	1.23178E 00	1.03520E 00	1.05478E 00
5.27773E 00	1.25423E 00	9.53218E-02	1.16796E 00	1.23200E 00	1.03508E 00	1.05482E 00
5.33715E 00	1.25431E 00	9.45396E-02	1.16800E 00	1.23203E 00	1.03510E 00	1.05482E 00
5.39656E 00	1.25438E 00	9.37572E-02	1.16804E 00	1.23206E 00	1.03511E 00	1.05481E 00
5.45597E 00	1.25449E 00	9.29740E-02	1.16803E 00	1.23203E 00	1.03516E 00	1.05479E 00
5.51538E 00	1.25460E 00	9.21906E-02	1.16802E 00	1.23200E 00	1.03522E 00	1.05477E 00
5.57480E 00	1.25465E 00	9.16386E-02	1.16805E 00	1.23203E 00	1.03523E 00	1.05477E 00

M_∞ = 1.2 (Concluded)

R	U	V	RHO	P	M	T
5.63421E 00	1.25470E 00	9.10876E-02	1.16809E 00	1.23206E 00	1.03524E 00	1.05477E 00
5.69362E 00	1.25479E 00	9.06108E-02	1.16808E 00	1.23203E 00	1.03529E 00	1.05475E 00
5.75304E 00	1.25487E 00	9.01349E-02	1.16807E 00	1.23200E 00	1.03534E 00	1.05473E 00
5.81245E 00	1.25511E 00	8.96497E-02	1.16791E 00	1.23175E 00	1.03554E 00	1.05466E 00
5.87186E 00	1.25534E 00	8.91656E-02	1.16775E 00	1.23150E 00	1.03574E 00	1.05459E 00
5.93128E 00	1.25557E 00	8.86811E-02	1.16759E 00	1.23125E 00	1.03593E 00	1.05452E 00
5.99069E 00	1.25581E 00	8.81965E-02	1.16743E 00	1.23100E 00	1.03613E 00	1.05445E 00
6.05010E 00	1.25587E 00	8.76745E-02	1.16744E 00	1.23100E 00	1.03615E 00	1.05444E 00
6.10951E 00	1.25593E 00	8.71537E-02	1.16745E 00	1.23100E 00	1.03618E 00	1.05443E 00
6.16893E 00	1.25598E 00	8.66465E-02	1.16746E 00	1.23100E 00	1.03620E 00	1.05442E 00
6.22834E 00	1.25604E 00	8.61405E-02	1.16747E 00	1.23100E 00	1.03622E 00	1.05441E 00
6.28775E 00	1.25609E 00	8.56794E-02	1.16748E 00	1.23100E 00	1.03624E 00	1.05441E 00
6.34717E 00	1.25615E 00	8.52183E-02	1.16749E 00	1.23100E 00	1.03627E 00	1.05440E 00
6.40658E 00	1.25620E 00	8.48007E-02	1.16750E 00	1.23100E 00	1.03629E 00	1.05439E 00
6.46599E 00	1.25625E 00	8.43833E-02	1.16751E 00	1.23100E 00	1.03631E 00	1.05438E 00
6.52540E 00	1.25646E 00	8.40669E-02	1.16734E 00	1.23075E 00	1.03650E 00	1.05432E 00
6.58482E 00	1.25667E 00	8.37505E-02	1.16718E 00	1.23050E 00	1.03668E 00	1.05425E 00
6.64423E 00	1.25688E 00	8.34113E-02	1.16702E 00	1.23025E 00	1.03687E 00	1.05418E 00
6.70364E 00	1.25709E 00	8.30721E-02	1.16685E 00	1.23000E 00	1.03706E 00	1.05412E 00
6.76306E 00	1.25714E 00	8.25486E-02	1.16686E 00	1.23000E 00	1.03707E 00	1.05411E 00
6.82247E 00	1.25718E 00	8.20250E-02	1.16687E 00	1.23000E 00	1.03709E 00	1.05410E 00
6.88188E 00	1.25723E 00	8.14889E-02	1.16687E 00	1.23000E 00	1.03710E 00	1.05410E 00
6.94130E 00	1.25728E 00	8.09540E-02	1.16688E 00	1.23000E 00	1.03712E 00	1.05410E 00
7.00071E 00	1.25732E 00	8.05477E-02	1.16688E 00	1.23000E 00	1.03713E 00	1.05409E 00
7.06012E 00	1.25736E 00	8.01416E-02	1.16689E 00	1.23000E 00	1.03714E 00	1.05409E 00
7.11953E 00	1.25739E 00	7.97703E-02	1.16689E 00	1.23000E 00	1.03715E 00	1.05408E 00
7.17895E 00	1.25743E 00	7.94003E-02	1.16689E 00	1.23000E 00	1.03716E 00	1.05408E 00
7.23836E 00	1.25780E 00	7.90478E-02	1.16656E 00	1.22950E 00	1.03751E 00	1.05395E 00
7.29777E 00	1.25818E 00	7.86951E-02	1.16622E 00	1.22900E 00	1.03786E 00	1.05383E 00
7.35719E 00	1.25855E 00	7.83145E-02	1.16589E 00	1.22850E 00	1.03821E 00	1.05370E 00
7.41660E 00	1.25892E 00	7.79336E-02	1.16555E 00	1.22800E 00	1.03856E 00	1.05358E 00
7.47601E 00	1.25930E 00	7.74709E-02	1.16521E 00	1.22750E 00	1.03891E 00	1.05345E 00
7.53543E 00	1.25968E 00	7.70078E-02	1.16488E 00	1.22700E 00	1.03926E 00	1.05333E 00
7.59484E 00	1.26005E 00	7.65168E-02	1.16454E 00	1.22650E 00	1.03960E 00	1.05320E 00
7.65425E 00	1.26043E 00	7.60254E-02	1.16420E 00	1.22600E 00	1.03995E 00	1.05308E 00
7.71366E 00	1.26081E 00	7.55336E-02	1.16386E 00	1.22550E 00	1.04030E 00	1.05296E 00
7.77308E 00	1.26118E 00	7.50427E-02	1.16352E 00	1.22500E 00	1.04064E 00	1.05283E 00
7.83249E 00	1.26155E 00	7.45779E-02	1.16319E 00	1.22450E 00	1.04099E 00	1.05271E 00
7.89200E 00	1.26192E 00	7.41128E-02	1.16285E 00	1.22400E 00	1.04133E 00	1.05259E 00

$M_\infty = 1.3$

R	U	V	RHO	P	M	T
1.00000E 00	1.89100E 00	0.0	5.88477E-01	4.80000E-01	1.76958E 00	8.15665E-01
1.03976E 00	1.84244E 00	5.51073E-02	6.45235E-01	5.42500E-01	1.69895E 00	8.40779E-01
1.07952E 00	1.79105E 00	1.07142E-01	6.98702E-01	6.05000E-01	1.62962E 00	8.65892E-01
1.11927E 00	1.73689E 00	1.55854E-01	7.49154E-01	6.67500E-01	1.56138E 00	8.91005E-01
1.15903E 00	1.68000E 00	2.01000E-01	7.96840E-01	7.30000E-01	1.49402E 00	9.16119E-01
1.19879E 00	1.65507E 00	2.10133E-01	8.33872E-01	7.73250E-01	1.46425E 00	9.27300E-01
1.23855E 00	1.62977E 00	2.18851E-01	8.70023E-01	8.16500E-01	1.43460E 00	9.38481E-01
1.27830E 00	1.60408E 00	2.27143E-01	9.05321E-01	8.59750E-01	1.40504E 00	9.49663E-01
1.31806E 00	1.57800E 00	2.35000E-01	9.39799E-01	9.03000E-01	1.37556E 00	9.60844E-01
1.35782E 00	1.55883E 00	2.36723E-01	9.60071E-01	9.30500E-01	1.35357E 00	9.69199E-01
1.39758E 00	1.53945E 00	2.38299E-01	9.79997E-01	9.58000E-01	1.33160E 00	9.77553E-01
1.43734E 00	1.51984E 00	2.39726E-01	9.99585E-01	9.85499E-01	1.30964E 00	9.85908E-01
1.47709E 00	1.50000E 00	2.41000E-01	1.01884E 00	1.01300E 00	1.28769E 00	9.94264E-01
1.51685E 00	1.48594E 00	2.40326E-01	1.03177E 00	1.03200E 00	1.27203E 00	1.00022E 00
1.55661E 00	1.47176E 00	2.39602E-01	1.04454E 00	1.05100E 00	1.25636E 00	1.00618E 00
1.59637E 00	1.45745E 00	2.38827E-01	1.05717E 00	1.07000E 00	1.24069E 00	1.01214E 00
1.63612E 00	1.44300E 00	2.37999E-01	1.06964E 00	1.08900E 00	1.22500E 00	1.01810E 00
1.67588E 00	1.43482E 00	2.36509E-01	1.08002E 00	1.10325E 00	1.21600E 00	1.02151E 00
1.71564E 00	1.42660E 00	2.35012E-01	1.09032E 00	1.11750E 00	1.20699E 00	1.02493E 00
1.75540E 00	1.41832E 00	2.33508E-01	1.10056E 00	1.13175E 00	1.19798E 00	1.02834E 00
1.79515E 00	1.41000E 00	2.32000E-01	1.11073E 00	1.14600E 00	1.18896E 00	1.03176E 00
1.83491E 00	1.40256E 00	2.29998E-01	1.11757E 00	1.15650E 00	1.18082E 00	1.03483E 00
1.87467E 00	1.39509E 00	2.27997E-01	1.12438E 00	1.16700E 00	1.17268E 00	1.03791E 00
1.91443E 00	1.38756E 00	2.25998E-01	1.13114E 00	1.17750E 00	1.16453E 00	1.04099E 00
1.95419E 00	1.38000E 00	2.24000E-01	1.13786E 00	1.18800E 00	1.15638E 00	1.04406E 00
1.99394E 00	1.37504E 00	2.21486E-01	1.14348E 00	1.19625E 00	1.15084E 00	1.04615E 00
2.03370E 00	1.37005E 00	2.18983E-01	1.14908E 00	1.20450E 00	1.14530E 00	1.04823E 00
2.07346E 00	1.36504E 00	2.16486E-01	1.15465E 00	1.21275E 00	1.13976E 00	1.05031E 00
2.11322E 00	1.36000E 00	2.14000E-01	1.16021E 00	1.22100E 00	1.13422E 00	1.05240E 00
2.15297E 00	1.35751E 00	2.11993E-01	1.16496E 00	1.22725E 00	1.13136E 00	1.05347E 00
2.19273E 00	1.35502E 00	2.09991E-01	1.16970E 00	1.23350E 00	1.12850E 00	1.05454E 00
2.23249E 00	1.35251E 00	2.07993E-01	1.17443E 00	1.23975E 00	1.12564E 00	1.05562E 00
2.27225E 00	1.35000E 00	2.06001E-01	1.17915E 00	1.24600E 00	1.12278E 00	1.05669E 00
2.31201E 00	1.34751E 00	2.04244E-01	1.18342E 00	1.25175E 00	1.11998E 00	1.05774E 00
2.35176E 00	1.34501E 00	2.02492E-01	1.18768E 00	1.25750E 00	1.11719E 00	1.05878E 00
2.39152E 00	1.34251E 00	2.00743E-01	1.19193E 00	1.26325E 00	1.11439E 00	1.05983E 00
2.43128E 00	1.34000E 00	1.98999E-01	1.19618E 00	1.26900E 00	1.11159E 00	1.06088E 00
2.47104E 00	1.33826E 00	1.97244E-01	1.19886E 00	1.27275E 00	1.10957E 00	1.06164E 00
2.51079E 00	1.33651E 00	1.95493E-01	1.20153E 00	1.27650E 00	1.10755E 00	1.06239E 00

M_∞ = 1.3 (Continued)

R	U	V	RHO	P	M	T
2.55055E 00	1.33476E 00	1.93744E-01	1.20421E 00	1.28025E 00	1.10553E 00	1.06314E 00
2.59031E 00	1.33300E 00	1.92000E-01	1.20688E 00	1.28400E 00	1.10350E 00	1.06390E 00
2.63007E 00	1.33225E 00	1.90247E-01	1.20974E 00	1.28750E 00	1.10250E 00	1.06427E 00
2.66982E 00	1.33150E 00	1.88497E-01	1.21260E 00	1.29100E 00	1.10150E 00	1.06465E 00
2.70958E 00	1.33075E 00	1.86747E-01	1.21546E 00	1.29450E 00	1.10050E 00	1.06502E 00
2.74934E 00	1.33000E 00	1.85000E-01	1.21832E 00	1.29800E 00	1.09949E 00	1.06540E 00
2.78910E 00	1.32900E 00	1.83247E-01	1.21920E 00	1.29950E 00	1.09825E 00	1.06586E 00
2.82886E 00	1.32801E 00	1.81496E-01	1.22008E 00	1.30100E 00	1.09701E 00	1.06633E 00
2.86861E 00	1.32700E 00	1.79747E-01	1.22095E 00	1.30250E 00	1.09576E 00	1.06679E 00
2.90837E 00	1.32600E 00	1.77999E-01	1.22183E 00	1.30400E 00	1.09452E 00	1.06725E 00
2.94813E 00	1.32475E 00	1.76746E-01	1.22287E 00	1.30575E 00	1.09310E 00	1.06778E 00
2.98789E 00	1.32350E 00	1.75495E-01	1.22390E 00	1.30750E 00	1.09169E 00	1.06831E 00
3.02764E 00	1.32225E 00	1.74246E-01	1.22493E 00	1.30925E 00	1.09027E 00	1.06884E 00
3.06740E 00	1.32100E 00	1.72999E-01	1.22596E 00	1.31100E 00	1.08885E 00	1.06936E 00
3.10716E 00	1.32075E 00	1.71999E-01	1.22790E 00	1.31325E 00	1.08847E 00	1.06950E 00
3.14692E 00	1.32050E 00	1.70998E-01	1.22984E 00	1.31550E 00	1.08809E 00	1.06964E 00
3.18668E 00	1.32025E 00	1.69998E-01	1.23178E 00	1.31775E 00	1.08771E 00	1.06979E 00
3.22643E 00	1.32000E 00	1.69000E-01	1.23373E 00	1.32000E 00	1.08733E 00	1.06993E 00
3.26619E 00	1.32000E 00	1.67750E-01	1.23412E 00	1.32050E 00	1.08718E 00	1.06999E 00
3.30595E 00	1.32000E 00	1.66500E-01	1.23452E 00	1.32100E 00	1.08702E 00	1.07005E 00
3.34571E 00	1.32000E 00	1.65250E-01	1.23492E 00	1.32150E 00	1.08686E 00	1.07010E 00
3.38546E 00	1.32000E 00	1.63999E-01	1.23532E 00	1.32200E 00	1.08670E 00	1.07016E 00
3.42522E 00	1.31925E 00	1.62747E-01	1.23680E 00	1.32400E 00	1.08580E 00	1.07050E 00
3.46498E 00	1.31850E 00	1.61497E-01	1.23828E 00	1.32600E 00	1.08490E 00	1.07083E 00
3.50474E 00	1.31775E 00	1.60248E-01	1.23976E 00	1.32800E 00	1.08400E 00	1.07117E 00
3.54449E 00	1.31700E 00	1.59000E-01	1.24124E 00	1.33000E 00	1.08309E 00	1.07151E 00
3.58425E 00	1.31625E 00	1.58249E-01	1.24112E 00	1.33025E 00	1.08226E 00	1.07182E 00
3.62401E 00	1.31550E 00	1.57498E-01	1.24099E 00	1.33050E 00	1.08142E 00	1.07213E 00
3.66377E 00	1.31475E 00	1.56748E-01	1.24086E 00	1.33075E 00	1.08058E 00	1.07244E 00
3.70353E 00	1.31400E 00	1.55999E-01	1.24073E 00	1.33100E 00	1.07974E 00	1.07275E 00
3.74328E 00	1.31350E 00	1.54998E-01	1.24094E 00	1.33150E 00	1.07913E 00	1.07298E 00
3.78304E 00	1.31300E 00	1.53998E-01	1.24114E 00	1.33200E 00	1.07852E 00	1.07321E 00
3.82280E 00	1.31250E 00	1.52998E-01	1.24134E 00	1.33250E 00	1.07790E 00	1.07344E 00
3.86256E 00	1.31200E 00	1.52000E-01	1.24154E 00	1.33300E 00	1.07728E 00	1.07366E 00
3.90231E 00	1.31175E 00	1.51250E-01	1.24186E 00	1.33350E 00	1.07695E 00	1.07379E 00
3.94207E 00	1.31150E 00	1.50500E-01	1.24219E 00	1.33400E 00	1.07662E 00	1.07391E 00
3.98183E 00	1.31125E 00	1.49750E-01	1.24251E 00	1.33450E 00	1.07628E 00	1.07404E 00
4.02159E 00	1.31100E 00	1.49000E-01	1.24283E 00	1.33500E 00	1.07595E 00	1.07416E 00
4.06135E 00	1.31075E 00	1.48250E-01	1.24292E 00	1.33525E 00	1.07561E 00	1.07428E 00

M_∞ = 1.3 (Concluded)

R	U	V	RHO	P	M	T
4.10110E 00	1.31050E 00	1.47499E-01	1.24301E 00	1.33550E 00	1.07528E 00	1.07441E 00
4.14086E 00	1.31025E 00	1.46749E-01	1.24310E 00	1.33575E 00	1.07495E 00	1.07453E 00
4.18062E 00	1.31000E 00	1.45999E-01	1.24319E 00	1.33600E 00	1.07462E 00	1.07465E 00
4.22038E 00	1.31000E 00	1.44999E-01	1.24361E 00	1.33650E 00	1.07451E 00	1.07469E 00
4.26013E 00	1.31000E 00	1.43999E-01	1.24403E 00	1.33700E 00	1.07440E 00	1.07473E 00
4.29989E 00	1.31000E 00	1.43000E-01	1.24444E 00	1.33750E 00	1.07429E 00	1.07478E 00
4.33965E 00	1.31000E 00	1.42000E-01	1.24486E 00	1.33800E 00	1.07418E 00	1.07482E 00
4.37941E 00	1.31000E 00	1.41249E-01	1.24529E 00	1.33850E 00	1.07410E 00	1.07485E 00
4.41916E 00	1.31000E 00	1.40500E-01	1.24572E 00	1.33900E 00	1.07402E 00	1.07488E 00
4.45892E 00	1.31000E 00	1.39749E-01	1.24615E 00	1.33950E 00	1.07394E 00	1.07491E 00
4.49868E 00	1.31000E 00	1.39000E-01	1.24658E 00	1.34000E 00	1.07386E 00	1.07493E 00
4.53844E 00	1.31000E 00	1.38249E-01	1.24655E 00	1.34000E 00	1.07378E 00	1.07496E 00
4.57820E 00	1.31000E 00	1.37500E-01	1.24652E 00	1.34000E 00	1.07370E 00	1.07499E 00
4.61795E 00	1.31000E 00	1.36749E-01	1.24648E 00	1.34000E 00	1.07362E 00	1.07502E 00
4.65771E 00	1.31000E 00	1.36000E-01	1.24645E 00	1.34000E 00	1.07354E 00	1.07505E 00
4.69747E 00	1.31025E 00	1.35499E-01	1.24677E 00	1.34025E 00	1.07374E 00	1.07498E 00
4.73723E 00	1.31050E 00	1.35000E-01	1.24709E 00	1.34050E 00	1.07394E 00	1.07490E 00
4.77698E 00	1.31075E 00	1.34500E-01	1.24740E 00	1.34075E 00	1.07414E 00	1.07483E 00
4.81674E 00	1.31100E 00	1.34000E-01	1.24772E 00	1.34100E 00	1.07434E 00	1.07476E 00
4.85650E 00	1.31125E 00	1.33250E-01	1.24780E 00	1.34100E 00	1.07451E 00	1.07469E 00
4.89626E 00	1.31150E 00	1.32501E-01	1.24787E 00	1.34100E 00	1.07468E 00	1.07463E 00
4.93602E 00	1.31175E 00	1.31751E-01	1.24795E 00	1.34100E 00	1.07486E 00	1.07456E 00
4.97577E 00	1.31200E 00	1.31000E-01	1.24802E 00	1.34100E 00	1.07503E 00	1.07450E 00
5.01553E 00	1.31225E 00	1.30500E-01	1.24811E 00	1.34100E 00	1.07523E 00	1.07443E 00
5.05529E 00	1.31250E 00	1.30000E-01	1.24819E 00	1.34100E 00	1.07543E 00	1.07435E 00
5.09505E 00	1.31275E 00	1.29500E-01	1.24828E 00	1.34100E 00	1.07563E 00	1.07428E 00
5.13480E 00	1.31300E 00	1.28999E-01	1.24836E 00	1.34100E 00	1.07583E 00	1.07420E 00
5.17456E 00	1.31325E 00	1.28499E-01	1.24798E 00	1.34050E 00	1.07603E 00	1.07413E 00
5.21432E 00	1.31350E 00	1.27999E-01	1.24761E 00	1.34000E 00	1.07623E 00	1.07405E 00
5.25408E 00	1.31375E 00	1.27499E-01	1.24723E 00	1.33950E 00	1.07643E 00	1.07398E 00
5.29383E 00	1.31400E 00	1.26999E-01	1.24685E 00	1.33900E 00	1.07663E 00	1.07391E 00
5.33359E 00	1.31425E 00	1.26499E-01	1.24694E 00	1.33900E 00	1.07683E 00	1.07383E 00
5.37335E 00	1.31450E 00	1.26000E-01	1.24702E 00	1.33900E 00	1.07703E 00	1.07376E 00
5.41311E 00	1.31475E 00	1.25499E-01	1.24711E 00	1.33900E 00	1.07724E 00	1.07368E 00
5.45287E 00	1.31500E 00	1.25000E-01	1.24720E 00	1.33900E 00	1.07744E 00	1.07361E 00
5.49262E 00	1.31525E 00	1.24500E-01	1.24705E 00	1.33875E 00	1.07764E 00	1.07353E 00
5.53238E 00	1.31550E 00	1.24000E-01	1.24690E 00	1.33850E 00	1.07784E 00	1.07346E 00
5.57214E 00	1.31575E 00	1.23500E-01	1.24676E 00	1.33825E 00	1.07804E 00	1.07338E 00
5.61200E 00	1.31600E 00	1.23000E-01	1.24661E 00	1.33800E 00	1.07825E 00	1.07331E 00

$M_\infty = 1.122$

R	U	V	RHO	P	M	T
1.000000E 00	1.77200E 00	0.0	5.65018E-01	4.50000E-01	1.67813E 00	7.96434E-01
1.35172E 00	1.45000E 00	2.04000E-01	8.63997E-01	8.13000E-01	1.27813E 00	9.37503E-01
1.70345E 00	1.34000E 00	1.91000E-01	9.77892E-01	9.60000E-01	1.15456E 00	9.81704E-01
2.05517E 00	1.27500E 00	1.69999E-01	1.03292E 00	1.04000E 00	1.08340E 00	1.00686E 00
2.40689E 00	1.24500E 00	1.46000E-01	1.06122E 00	1.08100E 00	1.04969E 00	1.01864E 00
2.75862E 00	1.23200E 00	1.29999E-01	1.08417E 00	1.11000E 00	1.03475E 00	1.02383E 00
3.11034E 00	1.23000E 00	1.18000E-01	1.09274E 00	1.12000E 00	1.03153E 00	1.02495E 00
3.46207E 00	1.22200E 00	1.08000E-01	1.09917E 00	1.13000E 00	1.02256E 00	1.02804E 00
3.81379E 00	1.22000E 00	9.90005E-02	1.10593E 00	1.13800E 00	1.01980E 00	1.02900E 00
4.16551E 00	1.22000E 00	9.09997E-02	1.10764E 00	1.14000E 00	1.01917E 00	1.02921E 00
4.51724E 00	1.21500E 00	8.40002E-02	1.11045E 00	1.14500E 00	1.01367E 00	1.03111E 00
4.86896E 00	1.21500E 00	7.80005E-02	1.11321E 00	1.14800E 00	1.01327E 00	1.03125E 00
5.22068E 00	1.21600E 00	7.30001E-02	1.11347E 00	1.14800E 00	1.01395E 00	1.03101E 00
5.57241E 00	1.21800E 00	6.79997E-02	1.11216E 00	1.14600E 00	1.01567E 00	1.03042E 00
5.92413E 00	1.22000E 00	6.50004E-02	1.11188E 00	1.14500E 00	1.01751E 00	1.02979E 00
6.27586E 00	1.22000E 00	6.20004E-02	1.10988E 00	1.14300E 00	1.01735E 00	1.02984E 00
6.62758E 00	1.22100E 00	5.99999E-02	1.10827E 00	1.14100E 00	1.01825E 00	1.02953E 00
6.97930E 00	1.22300E 00	5.70004E-02	1.10799E 00	1.14000E 00	1.02011E 00	1.02885E 00
7.33103E 00	1.22500E 00	5.50001E-02	1.10870E 00	1.14000E 00	1.02203E 00	1.02823E 00
7.68275E 00	1.22600E 00	5.30000E-02	1.10904E 00	1.14000E 00	1.02295E 00	1.02791E 00
8.03447E 00	1.22700E 00	5.10003E-02	1.10939E 00	1.14000E 00	1.02387E 00	1.02759E 00
8.38620E 00	1.22800E 00	4.94994E-02	1.10779E 00	1.13800E 00	1.02481E 00	1.02727E 00
8.73792E 00	1.23000E 00	4.79995E-02	1.10560E 00	1.13500E 00	1.02677E 00	1.02659E 00
9.08964E 00	1.23000E 00	4.65001E-02	1.10168E 00	1.13100E 00	1.02671E 00	1.02661E 00
9.44137E 00	1.23100E 00	4.50004E-02	1.10106E 00	1.13000E 00	1.02766E 00	1.02628E 00
9.79309E 00	1.23200E 00	4.39996E-02	1.10142E 00	1.13000E 00	1.02863E 00	1.02594E 00
1.01448E 01	1.23300E 00	4.29996E-02	1.10178E 00	1.13000E 00	1.02961E 00	1.02561E 00
1.04965E 01	1.23400E 00	4.20004E-02	1.10215E 00	1.13000E 00	1.03058E 00	1.02527E 00
1.08483E 01	1.23500E 00	4.09995E-02	1.09958E 00	1.12700E 00	1.03156E 00	1.02493E 00
1.12000E 01	1.23700E 00	4.10004E-02	1.09838E 00	1.12500E 00	1.03358E 00	1.02423E 00

$M_\infty = 1.42$

R	U	V	RHO	P	M	T
1.00000E 00	1.98000E 00	0.0	5.96892E-01	4.95000E-01	1.83758E 00	8.29296E-01
1.11410E 00	1.82500E 00	1.98000E-01	7.67661E-01	6.96000E-01	1.62937E 00	9.06651E-01
1.22821E 00	1.71500E 00	2.42000E-01	8.88758E-01	8.52000E-01	1.49504E 00	9.58641E-01
1.34231E 00	1.64200E 00	2.65001E-01	9.93511E-01	9.85000E-01	1.41176E 00	9.91433E-01
1.45641E 00	1.59000E 00	2.77000E-01	1.06495E 00	1.08000E 00	1.35450E 00	1.01413E 00
1.57052E 00	1.54800E 00	2.79001E-01	1.11381E 00	1.15000E 00	1.30829E 00	1.03249E 00
1.68462E 00	1.51400E 00	2.77000E-01	1.15251E 00	1.20700E 00	1.27110E 00	1.04728E 00
1.79872E 00	1.49000E 00	2.72999E-01	1.18274E 00	1.25100E 00	1.24482E 00	1.05771E 00
1.91283E 00	1.46800E 00	2.68000E-01	1.20873E 00	1.29000E 00	1.22082E 00	1.06724E 00
2.02693E 00	1.45200E 00	2.62999E-01	1.22885E 00	1.32000E 00	1.20330E 00	1.07418E 00
2.14103E 00	1.44000E 00	2.57000E-01	1.24596E 00	1.34500E 00	1.18987E 00	1.07949E 00
2.25514E 00	1.43000E 00	2.52000E-01	1.26213E 00	1.36800E 00	1.17875E 00	1.08388E 00
2.36924E 00	1.42000E 00	2.47000E-01	1.27362E 00	1.38600E 00	1.16771E 00	1.08823E 00
2.48334E 00	1.41300E 00	2.42000E-01	1.28463E 00	1.40200E 00	1.15977E 00	1.09136E 00
2.59745E 00	1.41000E 00	2.37999E-01	1.29755E 00	1.41800E 00	1.15606E 00	1.09282E 00
2.71155E 00	1.40600E 00	2.32999E-01	1.30625E 00	1.43000E 00	1.15120E 00	1.09474E 00
2.82565E 00	1.40200E 00	2.28000E-01	1.31128E 00	1.43800E 00	1.14636E 00	1.09664E 00
2.93976E 00	1.40100E 00	2.24000E-01	1.31688E 00	1.44500E 00	1.14471E 00	1.09729E 00
3.05386E 00	1.40000E 00	2.21000E-01	1.32074E 00	1.45000E 00	1.14323E 00	1.09787E 00
3.16796E 00	1.40000E 00	2.17999E-01	1.32507E 00	1.45500E 00	1.14276E 00	1.09805E 00
3.28207E 00	1.39800E 00	2.14000E-01	1.32838E 00	1.46000E 00	1.14014E 00	1.09908E 00
3.39617E 00	1.39700E 00	2.12000E-01	1.32958E 00	1.46200E 00	1.13883E 00	1.09959E 00
3.51027E 00	1.39800E 00	2.08000E-01	1.33250E 00	1.46500E 00	1.13923E 00	1.09944E 00
3.62438E 00	1.39800E 00	2.05000E-01	1.33593E 00	1.46900E 00	1.13879E 00	1.09961E 00
3.73848E 00	1.39700E 00	2.02001E-01	1.33706E 00	1.47100E 00	1.13735E 00	1.10018E 00
3.85258E 00	1.39600E 00	1.98000E-01	1.33813E 00	1.47300E 00	1.13578E 00	1.10079E 00
3.96669E 00	1.39600E 00	1.96000E-01	1.33981E 00	1.47500E 00	1.13550E 00	1.10090E 00
4.08079E 00	1.39600E 00	1.93000E-01	1.34142E 00	1.47700E 00	1.13508E 00	1.10107E 00
4.19489E 00	1.39500E 00	1.90000E-01	1.34347E 00	1.48000E 00	1.13367E 00	1.10162E 00
4.30900E 00	1.39500E 00	1.87000E-01	1.34328E 00	1.48000E 00	1.13326E 00	1.10178E 00

$M_\infty = 1.6$

R	U	V	RHO	P	M	T
1.00000E 00	2.12300E 00	0.0	6.11805E-01	5.25400E-01	1.93619E 00	8.58771E-01
1.11100E 00	1.95700E 00	2.37000E-01	8.07147E-01	7.64000E-01	1.71245E 00	9.46543E-01
1.22200E 00	1.84500E 00	2.91899E-01	9.41536E-01	9.44000E-01	1.57664E 00	1.00262E 00
1.33300E 00	1.76600E 00	3.15999E-01	1.04144E 00	1.08400E 00	1.48619E 00	1.04086E 00
1.44400E 00	1.70800E 00	3.25799E-01	1.12219E 00	1.19900E 00	1.42170E 00	1.06845E 00
1.55500E 00	1.66700E 00	3.34000E-01	1.17730E 00	1.28000E 00	1.37802E 00	1.08724E 00
1.66599E 00	1.62800E 00	3.47700E-01	1.23089E 00	1.35900E 00	1.33899E 00	1.10408E 00
1.77699E 00	1.61000E 00	3.35001E-01	1.26892E 00	1.41300E 00	1.31708E 00	1.11354E 00
1.88799E 00	1.58900E 00	3.77000E-01	1.31301E 00	1.46900E 00	1.30489E 00	1.11881E 00
1.99899E 00	1.57200E 00	3.32000E-01	1.33521E 00	1.51000E 00	1.27688E 00	1.13091E 00
2.10999E 00	1.55700E 00	3.37000E-01	1.35700E 00	1.54300E 00	1.26262E 00	1.13707E 00
2.22099E 00	1.55000E 00	3.28200E-01	1.37602E 00	1.57000E 00	1.25359E 00	1.14097E 00
2.33199E 00	1.54200E 00	3.24600E-01	1.39588E 00	1.59800E 00	1.24472E 00	1.14480E 00
2.44299E 00	1.53300E 00	3.23000E-01	1.40575E 00	1.61500E 00	1.23531E 00	1.14886E 00
2.55399E 00	1.52700E 00	3.20000E-01	1.42048E 00	1.63600E 00	1.22867E 00	1.15172E 00
2.66499E 00	1.52500E 00	3.16000E-01	1.42938E 00	1.64800E 00	1.22583E 00	1.15294E 00
2.77599E 00	1.52100E 00	3.09400E-01	1.44211E 00	1.66600E 00	1.22048E 00	1.15525E 00
2.88698E 00	1.52200E 00	3.08000E-01	1.45115E 00	1.67600E 00	1.22120E 00	1.15494E 00
2.99798E 00	1.51500E 00	3.03600E-01	1.45555E 00	1.68600E 00	1.21334E 00	1.15833E 00
3.10898E 00	1.52000E 00	2.99999E-01	1.46824E 00	1.69800E 00	1.21761E 00	1.15649E 00
3.21998E 00	1.51500E 00	2.95299E-01	1.47019E 00	1.70400E 00	1.21171E 00	1.15903E 00
3.33098E 00	1.52000E 00	2.91800E-01	1.47774E 00	1.71000E 00	1.21601E 00	1.15718E 00
3.44200E 00	1.51700E 00	2.89199E-01	1.47755E 00	1.71200E 00	1.21253E 00	1.15868E 00

$M_\infty = 1.82$

R	U	V	RHO	P	M	T
1.00000E 00	2.29400E 00	0.0	6.18769E-01	5.57300E-01	2.04291E 00	9.00659E-01
1.03450E 00	2.15500E 00	2.31001E-01	7.80222E-01	7.65000E-01	1.84988E 00	9.80490E-01
1.16900E 00	2.05400E 00	3.03100E-01	9.24250E-01	9.56700E-01	1.72473E 00	1.03511E 00
1.25350E 00	1.97800E 00	3.50800E-01	1.02794E 00	1.10400E 00	1.63827E 00	1.07400E 00
1.33800E 00	1.91700E 00	3.78600E-01	1.12248E 00	1.24000E 00	1.57125E 00	1.10470E 00
1.42250E 00	1.87800E 00	4.02001E-01	1.20210E 00	1.35000E 00	1.53167E 00	1.12306E 00
1.50700E 00	1.83200E 00	4.18101E-01	1.25297E 00	1.43500E 00	1.48399E 00	1.14528E 00
1.59150E 00	1.81200E 00	4.24999E-01	1.30591E 00	1.50800E 00	1.46379E 00	1.15475E 00
1.67599E 00	1.78300E 00	4.26800E-01	1.35726E 00	1.58700E 00	1.43295E 00	1.16926E 00
1.76049E 00	1.76600E 00	4.34000E-01	1.38838E 00	1.63400E 00	1.41673E 00	1.17691E 00
1.84499E 00	1.74800E 00	4.35600E-01	1.43044E 00	1.69600E 00	1.39824E 00	1.18565E 00
1.92949E 00	1.73700E 00	4.35000E-01	1.45911E 00	1.73800E 00	1.38664E 00	1.19114E 00
2.01399E 00	1.72600E 00	4.33400E-01	1.49241E 00	1.78600E 00	1.37486E 00	1.19672E 00
2.09849E 00	1.71800E 00	4.31800E-01	1.51398E 00	1.81800E 00	1.36623E 00	1.20081E 00
2.18299E 00	1.70700E 00	4.33100E-01	1.53569E 00	1.85200E 00	1.35534E 00	1.20597E 00
2.26749E 00	1.70200E 00	4.30500E-01	1.55539E 00	1.88000E 00	1.34959E 00	1.20870E 00
2.35199E 00	1.69600E 00	4.27999E-01	1.57441E 00	1.90800E 00	1.34288E 00	1.21188E 00
2.43649E 00	1.69400E 00	4.26500E-01	1.58942E 00	1.92800E 00	1.34048E 00	1.21302E 00
2.52099E 00	1.68700E 00	4.24100E-01	1.60194E 00	1.94900E 00	1.33283E 00	1.21665E 00
2.60549E 00	1.69000E 00	4.21200E-01	1.61653E 00	1.96500E 00	1.33512E 00	1.21557E 00
2.68999E 00	1.68300E 00	4.18900E-01	1.63061E 00	1.98800E 00	1.32751E 00	1.21917E 00
2.77449E 00	1.68700E 00	4.16001E-01	1.64256E 00	2.00000E 00	1.33080E 00	1.21761E 00
2.85900E 00	1.68400E 00	4.13700E-01	1.65011E 00	2.01200E 00	1.32723E 00	1.21931E 00

APPENDIX B
ADDITIONAL DATA FOR M_∞ = 1.05, 1.1, 1.2, AND 1.5

Because AEDC data were consistently lower in shock standoff distance than predicted by theory in the low supersonic flow regime, additional shadowgraph and pressure data were obtained with the same testing setup in the Aerodynamic Wind Tunnel (1T) for M_∞ = 1.05, 1.1, 1.2, and 1.5 after the completion of the technical report. Therefore, the new data are included herein as an appendix.

In the additional experiments special attention was given to the optical lineup in taking shadowgraphs, and the area covered by the pictures was increased to 11 by 14 in. Figure B-1 shows the shadowgraphs.

A comparison of the present data with the theoretical results reported in the main text is given in Fig. B-2 for the shock standoff distance and in Fig. B-3 for the shock position. Two sets of data, one from each side of the model at different runs, were included for M_∞ = 1.2 only. It is seen that a better agreement between theory and experiment is obtained. No significant change in the surface pressure between the more recent data and the data shown in Fig. 2 for M_∞ = 1.05, 1.1, and 1.2 can be found. The more recent data, therefore, provide further evidence to confirm the conclusion presented in the main text.

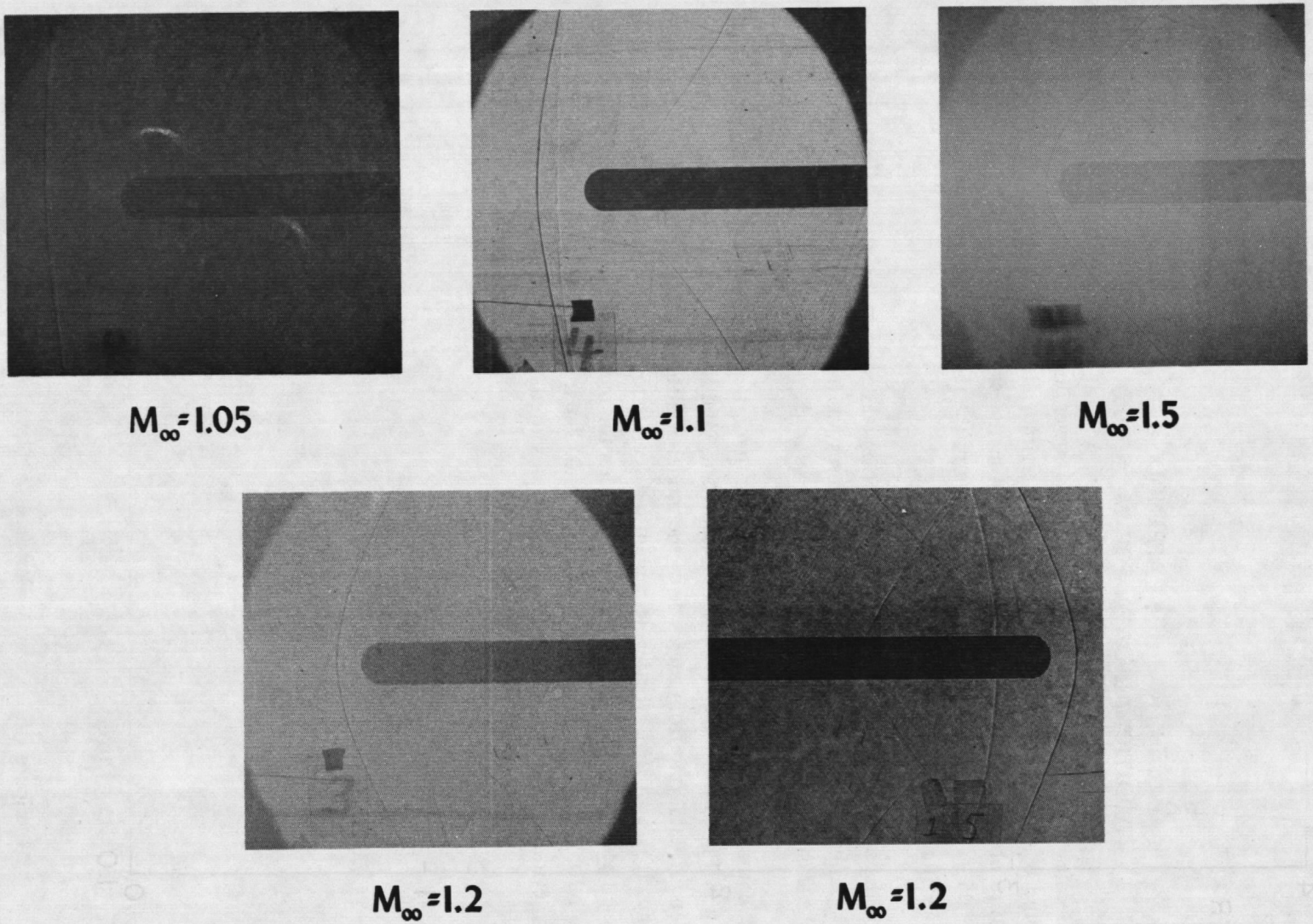

Figure B-1. Shadowgraphs of flow past hemisphere-cylinder at M_∞ = 1.05, 1.1, 1.2, and 1.5.

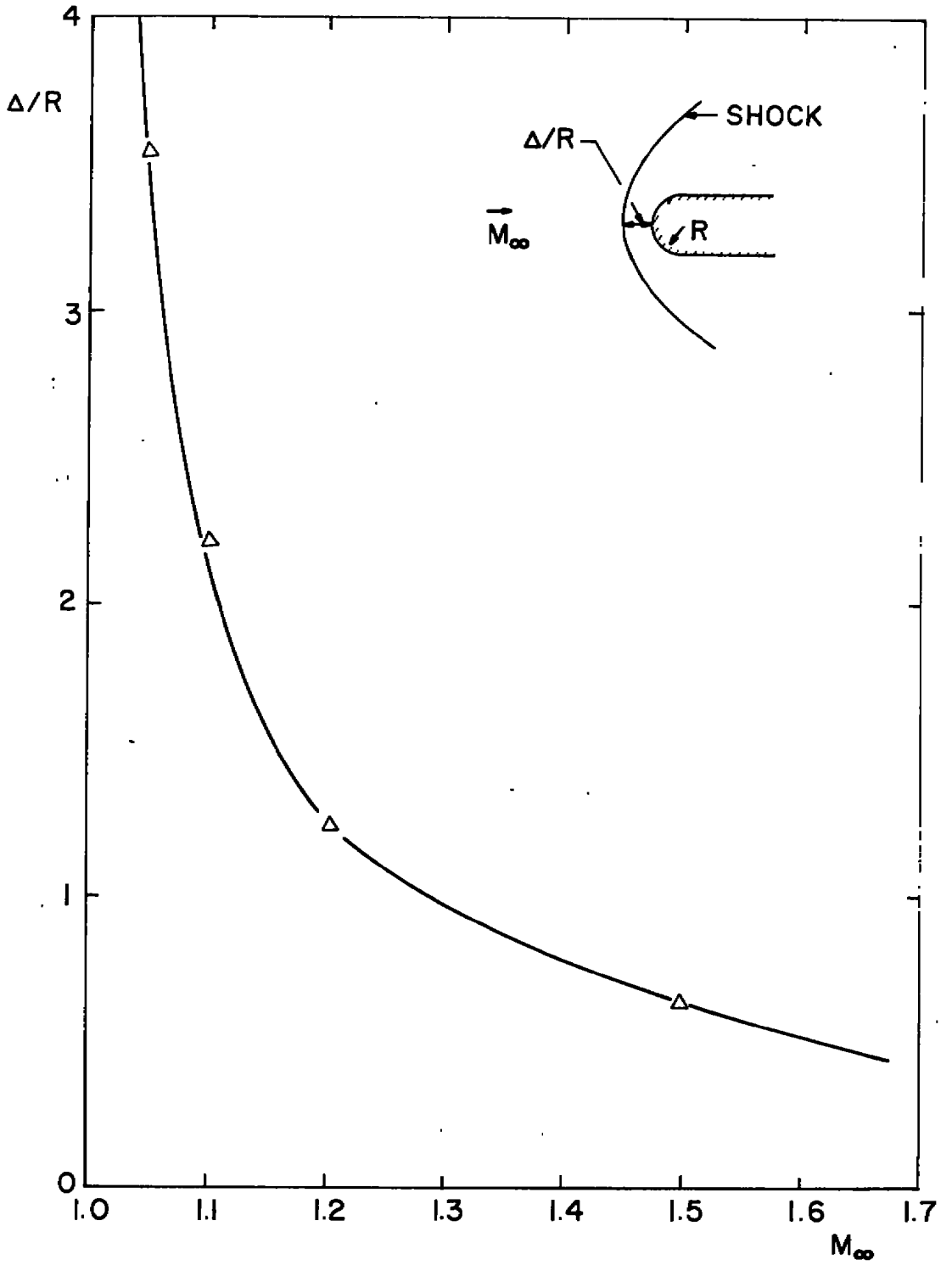

Figure B-2. Comparison of shock standoff distance between calculation and experiment.

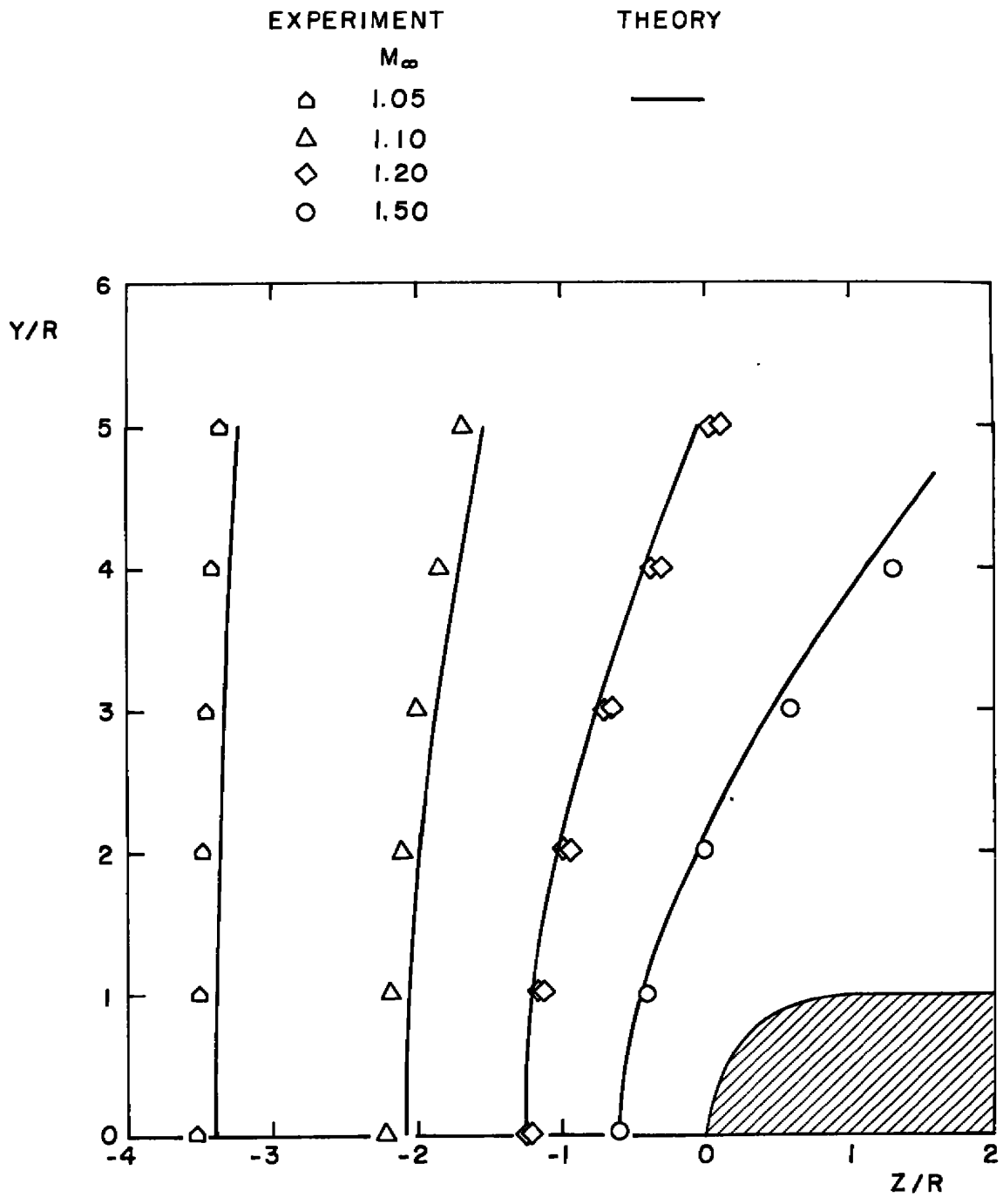

Figure B-3. Comparison of theoretical shock position with experiment, $\gamma = 1.4$.

NOMENCLATURE

a	Local speed of sound
C_p	Surface pressure coefficient
c_p	Specific heat of the gas at constant pressure
c_v	Specific heat of the gas at constant volume
K	Curvature of the body in the meridian plane
M	Mach number
n,s	Body-oriented coordinate system
P	Pressure
q	Total velocity
R	Radius of the cylinder
r,Y	Radial distance from the body axis
S	Entropy of the gas
u,v	Velocity components in the n and s directions, respectively
Z	Axial distance from the nosetip
γ	Specific heat ratio, c_p/c_v
Δ	Bow shock standoff distance
η,ξ	Coordinates in the computation plane
θ	Inclination angle of the body
κ	$1 + K n$
μ	Mach number
ρ	Density of the gas
ψ	Velocity potential
$()_\infty$	Subscript for free-stream conditions